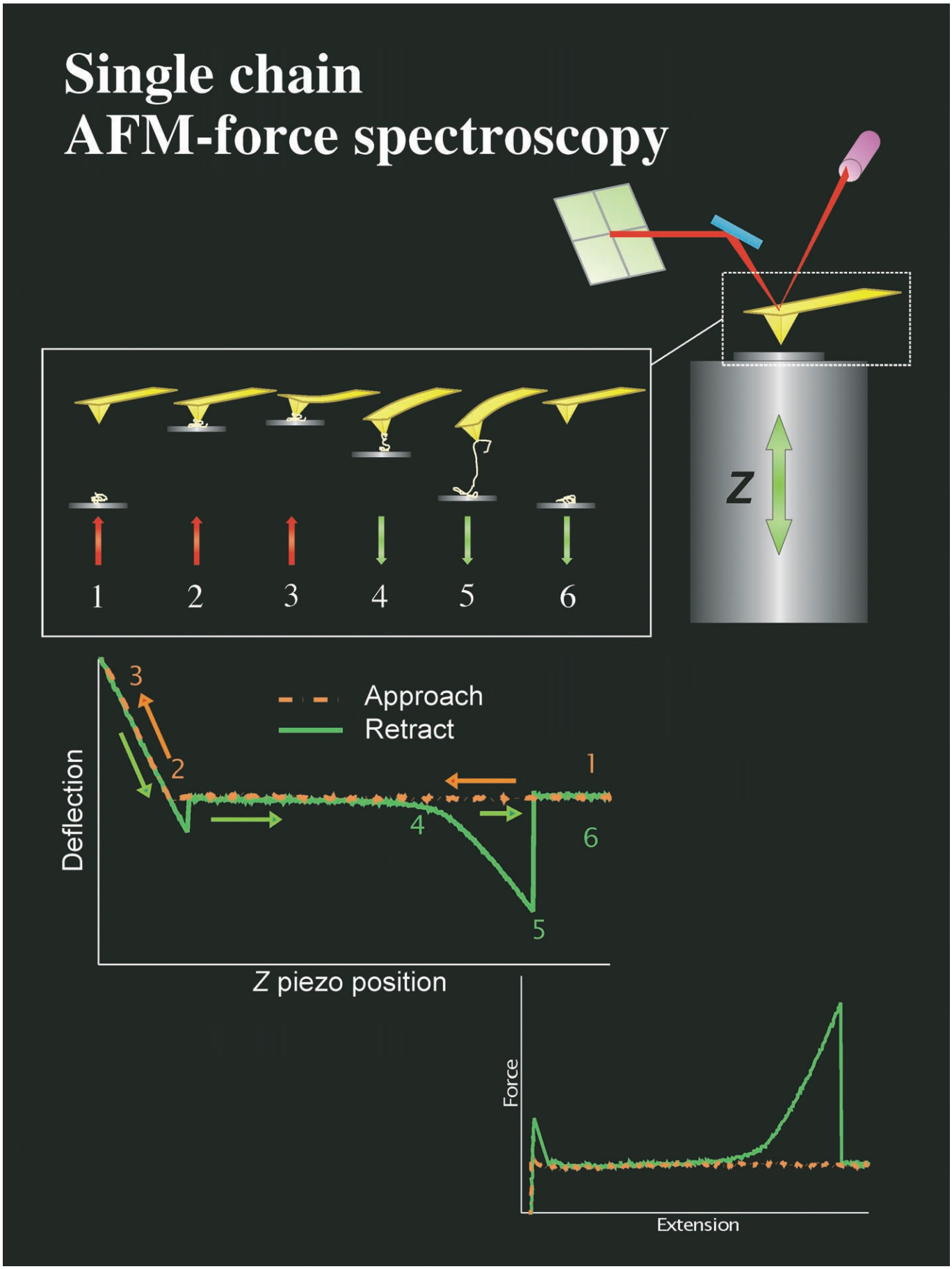

 DOI: 10.1002/cphc.200700175

DOI: 10.1002/cphc.200700175

Interrogation of Single Synthetic Polymer Chains and Polysaccharides by AFM-Based Force Spectroscopy**

Marina I. Giannotti and G. Julius Vancso*[a]

This contribution reviews selected mechanical experiments on individual flexible macromolecules using single-molecule force spectroscopy (SMFS) based on atomic force microscopy. Focus is placed on the analysis of elasticity and conformational changes in single polymer chains upon variation of the external environment, as well as on conformational changes induced by the mechanical stress applied to individual macromolecular chains. Various experimental strategies regarding single-molecule manipulation and SMFS testing are discussed, as is theoretical analysis through single-chain elasticity models derived from statistical mechanics. Moreover, a complete record, reported to date, of the parameters obtained when applying the models to fit experimental results on synthetic polymers and polysaccharides is presented.

1. Introduction

Every major step in nature involves mechanical movement at a single-molecule level. Also, the macroscopic properties of polymeric materials are closely related to the primary chemical composition, structure, conformation, and interactions at this level. Nanomechanical studies of single polymer chains contribute to the comprehension of fundamental aspects concerning the structural, mechanical, and binding properties of macromolecules. Understanding the elastic behavior, or deformation, of individual macromolecules is an essential issue in both (bio)polymer science and materials science.[1,2]

Single-molecule manipulation methods are particularly important in areas where temporal and spatial averaging is to be avoided, mechanical forces need to be measured, and individual species are to be tracked. The development of experimental tools has allowed the precise application and measurement of minute forces, thus opening new perspectives in life sciences as well as in materials science.[3–5] These tools have made possible observations of biological processes that could not otherwise be directly detected, for example, protein folding,[6–8] elasticity of macromolecules,[9–11] DNA mechanics,[12–16] mechanical work generated by motor proteins,[17–21] identification of individual molecules,[22,23] and binding potential of host–guest pairs.[10,24,25]

Single-molecule tools contribute to the discovery, identification, and description of temporally and spatially distinct states of a molecular species or of a complex process. They render it possible to follow, in real time and at an individual molecular level, the movements, forces, and strains developed during the course of a reaction, and even conformational changes induced by diverse means. The knowledge obtained through single-molecule experiments is primarily fundamental, and provides essential evidence for existing principles, as well as information regarding intra- and intermolecular interactions directly at the single-chain level.

Herein, we review selected mechanical experiments on individual flexible macromolecules using a technique based on atomic force microscopy (AFM), namely, single-molecule force spectroscopy (SMFS). Focus is placed on analyzing elasticity and conformational changes in single polymer chains while varying the external environment, as well as on the analysis of conformational changes induced by the mechanical stress applied to individual macromolecular chains. Many review articles have already been published on the use of SMFS for characterizing biomacromolecules, mainly DNA and proteins.[9,10,26–32] To complement and update the corresponding review literature, we focus here on the single-chain elasticity of synthetic polymers and polysaccharides, and on mechanically induced and external-stimulus-induced changes in conformation.

2. Single-Molecule Force Spectroscopy

The methods for single-molecule manipulation require two basic elements: a probe that can generate and detect forces and displacements, and a means of spatially locating the molecules. As reviewed by Clausen-Schaumann et al.[27] and Bustamante et al.,[4] various techniques are used for single-molecule manipulation and mechanical characterization according to the force range, minimum displacements, and applications, as well as practical advantages and disadvantages. Detectable forces can range from femtonewtons (fN) to a few nanonewtons

[a] *Dr. M. I. Giannotti, Prof. G. J. Vancso*
Department of Materials Science and Technology of Polymers and MESA+ Research Institute for Nanotechnology
University of Twente
P.O. Box 217, 7500 AE Enschede (The Netherlands)
Fax: (+31) 53489-3823
E-mail: G.J.Vancso@tnw.utwente.nl

[**] *AFM: Atomic Force Microscopy.*

(nN). Among the most commonly used tools, mechanical transducers and external field manipulators can be mentioned. Mechanical transducers, such as microneedles[33–35] and AFM-SMFS,[7,36,37] apply or sense forces through the displacement of a bendable beam. External field manipulators, for example, hydrodynamic flow and magnetic field (magnetic beads),[38,39] or light waves (photon fields, optical tweezers),[40–44] can be used to exert forces on macromolecules either by acting on the molecules themselves or by exerting forces through "handles", such as glass beads, polystyrene beads, or metallic particles attached to the molecules.

Table 1. An overview of single-molecule manipulation techniques.

Method	Force range [N]	Minimum displacement [m]	Application
Mechanical force (cantilevers)[a]	10^{-11}–10^{-7}	10^{-10}	DNA, proteins, polysaccharides, synthetic polymers
Mechanical force (microneedles)[a]	10^{-12}–10^{-10}	10^{-9}	Actin, stretching, unzipping, and twisting DNA
Flow field[b]	10^{-13}–10^{-9}	10^{-8}	DNA dynamics
Magnetic field[b]	10^{-14}–10^{-11}	10^{-8}	Stretching and twisting of DNA
Photon field[b]	10^{-13}–10^{-10}	10^{-9}	Actin, DNA, RNA, proteins, molecular motors

[a] Mechanical transducers: probes are bendable beams; spatial location occurs through beam deflection. [b] External field manipulators: probes are microscopic beads; spatial location occurs through bead displacement.

Bustamante et al.[4] summarized the force ranges and applications for these single-molecule manipulation methods (Table 1). AFM–SMFS, with forces higher than 10 pN, is most often used for the detection and mechanical characterization of DNA, proteins, polysaccharides, and synthetic polymers. The advantages of AFM–SMFS include its high spatial range sensitivity and versatility. Unlike biomembrane force probes, AFM–SMFS is not limited to the use of water as a medium, and makes use of organic solvents. This technique combines the possibility of locating and probing single molecules[45,46] under environmentally controlled conditions (solvent, temperature, salt, electrochemical potential, etc.).

Intermolecular and intramolecular interactions can be directly probed by AFM–SMFS, and the technique also allows the determination of molecular conformations by detecting molecular and supramolecular structures in biological macromolecules or in synthetic polymer systems. Moreover, the capability of AFM to resolve nanometer-sized details, together with its force detection sensitivity, have led to the development of molecular recognition imaging.[31] Through a combination of topographical imaging and force measurements, receptor sites can be localized with nanometer accuracy, thus rendering it possible to identify specific components in a complex biological sample while retaining its high-resolution imaging.

Colton and co-workers are considered the first to describe an experimental approach using force spectroscopy to determine the interaction between complementary strands of DNA and intrachain forces associated with the elasticity of single DNA strands.[12] In another early pioneering work, Gaub et al. described the use of force spectroscopy to determine intermolecular forces and energies between ligands and receptors, specifically between avidin (or streptavidin) and biotin analogues.[47] This new experimental platform has extended the understanding of molecular mechanisms in biological processes in life science and of material properties in soft matter physics. As summarized by Zhang et al.[48] and schematized in Figure 1, there are a great number of possibilities offered by this technique, in addition to single-chain elasticity measurements. These include: studies of melting and unzipping forces of double-stranded DNA;[12–16] protein unfolding;[6,8,32] interaction between macromolecules and solvents, that is, H-bonded structures in water;[49–52] interactions between polymers and other small molecules;[53–56] interfacial conformation and desorption forces;[57–68] and force-induced conformational transitions, such as the chair–boat transition of α-(1,4)- and α-(1,6)-linked polysaccharides,[69–84] some characteristic rotations of the exocyclic groups in β-(1,6)-linked polysaccharides,[77,85] and the rupture of secondary structures of individual polysaccharide chains and multistrand complexes.[55,80,86]

Marina Inés Giannotti was born in Mar del Plata, Argentina, in 1975. She graduated in Chemistry (1999) at the University of Mar del Plata, where she also received her Ph.D. in Materials Science (2004) with Prof. P. A. Oyanguren in the group of Prof. R. J. J. Williams (INTEMA/CONICET). In 2004 she was awarded a Marie Curie European postdoctoral fellowship and she moved to the University of Twente, The Netherlands, where she is working with Prof. G. J. Vancso on nanotechnology with single macromolecules using AFM-based single-molecule force spectroscopy.

Prof. G. Julius Vancso studied physics at the University of Budapest, Hungary, and materials science at the ETH-Zurich, and holds a Phd in solid state physics. Currently he is Professor and Chair of Polymer Materials Science and Technology at the University of Twente, MESA$^+$ Institute for Nanotechnology, in the Netherlands, and holds a visiting appointment with the Institute of Materials Research and Engineering in Singapore. His current research interests involve macromolecular nanotechnology, single-molecule studies (AFM, photonics), organometallic polymers, and surface engineering.

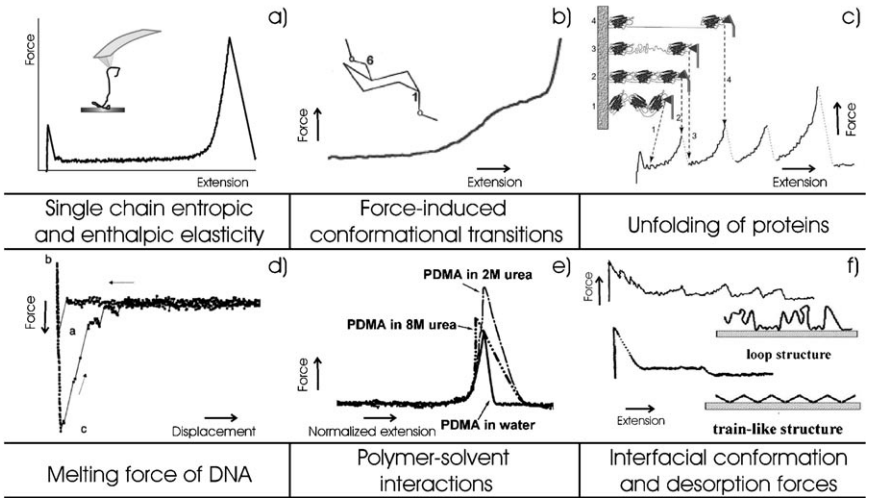

Figure 1. Examples of the use AFM–SMFS for studying intramolecular (a–c) and intermolecular (d–f) interactions in macromolecular systems. a) Single-chain entropic and enthalpic elasticity: schematics of a typical force–extension curve of a polymeric chain (see Section 3). b) Force-induced conformational transitions (see Section 4.1): "fingerprint" of elasticity for a linear polysaccharide [dextran: α-(1,6)-D-glucopyranose] ascribed to a chair-to-boat conformational transition of the pyranose ring combined with a rotation of the exocyclic group—the simplified monomeric unit is shown (adapted by permission from Macmillan Publishers Ltd: Nature Biotechnology,[73] copyright 2001). c) Unfolding of proteins: the saw-tooth pattern of peaks that is observed when force is applied to extend the protein corresponds to sequential unraveling of individual domains of a modular protein (adapted from ref. [32] with permission from Elsevier). d) Melting force of DNA: force versus displacement between complementary $(ACTG)_5$ and $(CAGT)_5$ functionalized surfaces (0.1 N NaCl, pH 7.0, 25 °C) (adapted from ref. [12] with permission from AAAS). e) Polymer–solvent/small-molecule interactions: normalized force–extension curves of single polydimethylacrylamide (PDMA) chain in different solvent conditions: aqueous solution, 2 and 8 M urea (reprinted in part with permission from ref. [56]. Copyright 2002 American Chemical Society). f) Interfacial conformation and adsorption force–force patterns for different adsorption conformations (adapted from ref. [87] with permission from Elsevier).

2.1. Principles of AFM-Based Single-Molecule Force Spectroscopy

The principles of AFM–SMFS have been extensively described in numerous articles.[10,11,23,25,28,87–93] In short, as shown in Figure 2a, a typical AFM–SMFS configuration includes an atomic force microscope, which is used to pick up and stretch single macromolecules. The chains can also be tethered to the microscope tip (AFM tip).[58,63,66,94] The force is measured through detection of the cantilever deflection by using the optical beam principle. Laser light is focused at the back of the cantilever, which is terminated by a sharp tip (typical radius values range from a few nanometers to a few tens of nanometers). The reflected light, and the corresponding deflection of the cantilever, is detected by a position-sensitive photodiode. For the force spectroscopy analysis, the macromolecular chains are physically or chemically adsorbed onto a solid substrate mounted on the piezoelectric tube, which can perform precise movements in the *z* direction.

Figure 2b schematically shows the movement of the piezoelectric positioner and the cantilever deflection during an approach–retract cycle. The chain extension can be obtained from the displacement of the piezo positioner (sample *z* position) corrected for the cantilever bend (Δz bending due to chain stretch). During an experiment, the cantilever initially stays free, as long as there are no long-range interactions (Figure 2b Position 1). Subsequently, the piezo moves towards the cantilever (approach; Figure 2b Position 2). While tip and sample are in contact, a force is applied to the sample, the cantilever is deflected upwards (positive deflection), and the macromolecules on the substrate can adsorb onto the tip (Figure 2b Position 3). Another strategy consists in the chemical tethering of polymer chains to the AFM tip (see Section 2.2). While tip and sample are in contact, the polymer molecules make a bridge adsorbing to the substrate. Upon separation of the tip and the substrate (retraction), the linking macromolecule is first uncoiled (Figure 2b Position 4) and stretched, which results in the deflection of the cantilever

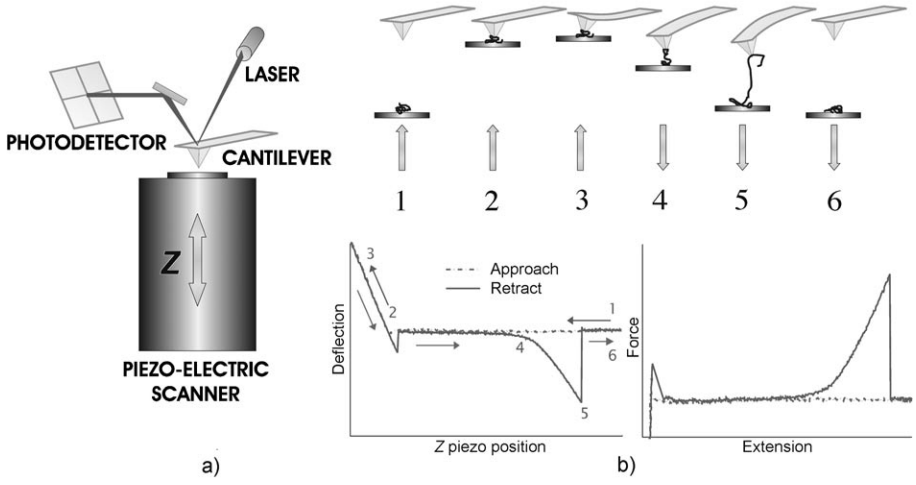

Figure 2. a) The principle of AFM-based SMFS and b) schematic illustration of a single-molecule deflection–displacement (piezo position) experiment.

towards the substrate (Figure 2b Position 5). A negative deflection is registered due to an attraction, and as the chain is further stretched, the weakest point of the structure breaks. In other words, the macromolecule desorbs either from the surface or from the tip, and the cantilever rapidly returns to its relaxed state (Figure 2b Position 6).

The deflection–displacement registered profile describes the elasticity of the macromolecule. The measured piezo position, z_0, can be converted into the actual distance between the AFM tip and the substrate (z, called "extension") by using Equation (1):

$$z = z_0 - 1/S \times D \quad (1)$$

Here, D is the measured cantilever deflection and S is the slope (voltage/length) of the recorded bending of the cantilever upon contacting and indenting the substrate surface (linear part of the curve). The cantilever deflection is then converted into force (F) by applying Hooke's law [Eq. (2)]:

$$F = -k_s \times (z - z_0) \quad (2)$$

where k_s is the spring constant of the cantilever. The minus sign in the equation is applied to transform the negative deflection into a positive force signal. Finally, the force (F) can be plotted against the extension (z), as shown in Figure 2b.

The cantilever spring constant k_s is normally determined by the thermal oscillation method,[95,96] but many other techniques, such as vibrational,[97–102] static loading,[100,103–107] and theoretical,[108–110] can be used. These methods are reviewed in detail by Hodges.[111] Here, we give a short summary of one of the most often used approaches, that is, the thermal oscillation technique. In the corresponding procedure, the cantilever is positioned far away from the sample, such that the cantilever only vibrates around its equilibrium position due to thermal fluctuations and is not affected by long-range forces. At a certain temperature T, the energy due to thermal motion of the air molecules causes the cantilever to oscillate with an amplitude x_0, so that [Eq. (3)]:

$$\left\langle \frac{1}{2} m \omega_0^2 x_0^2 \right\rangle = \frac{1}{2} k_B T \quad (3)$$

where m is the effective mass of the cantilever, ω_0 the resonant frequency, and k_B the Boltzmann constant. Since [Eq. (4)]:

$$\omega_0^2 = k_s/m \quad (4)$$

the spring constant k_s can be obtained as [Eq. (5)]:

$$k_s = k_B T / \langle x_0^2 \rangle \quad (5)$$

This result was obtained by Hutter and Bechhoefer[95] and does not take damping effects into account. The error in the value of the cantilever spring constant quoted in the original work was about 5%.

2.1.1. Force-Clamp AFM

In the regular AFM–SMFS experiments described above, the macromolecules are extended through vertical motion of the piezo positioner at a constant velocity while the resulting force is measured (i.e. the positioner is moved linearly as a function of time). In many cases (see Section 4), the force can drive the macromolecules into new conformational states by reducing the activation energy of conformations that are not populated at room temperature. However, when the molecule's end-to-end distance (extension) is controlled, the actual force applied to the polymer chain can usually not be predicted as it varies with the extension of the molecule in a complicated manner,[38,69,70] and is thus only known after the experiment. The group of Fernandez implemented force-clamp AFM to perform experiments either keeping the applied force constant at a set value (constant pulling force) or increasing it linearly over time (force-ramp mode), as well as using more complex wave forms (force-step mode). Thereby, they could study the stepwise unfolding of proteins[112] and capture conformational changes in polysaccharides.[75] In such cases, the entropic phase of the stretch cycle is completed quickly and the measurement can be focused on the postentropic events dominated by conformational transitions. Protein unfolding experiments using force-clamp AFM are summarized in a review by Samorì and co-workers.[113]

To control the force exerted on a macromolecule during stretching in force-ramp AFM, a feedback system compares the signal generated upon deflection of the AFM cantilever with computer-controlled set points and feeds the signal back to the piezoelectric positioner. The feedback system adjusts the length of the molecule being stretched by moving the piezoelectric stage in such a way that the molecule's tension (sensed by the cantilever deflection) corresponds to the predetermined value at each point during the stretching.

We need to comment briefly, at this juncture, about a possible nonequilibrium effect that may be caused by fast piezo retraction (i.e. bond loading) rates. In a force spectroscopy experiment chemical bonds (covalent, supramolecular, or adhesive bonds) are loaded and stressed upon increasing the tip–substrate distance bridged by the chain. In SMFS usually the rupture force value of the "weakest link" is measured. The force that is needed to rupture a chain is governed by thermomechanically activated bond dissociation kinetics and mechanochemistry.[114] For supramolecular bonds, for example, in associating polymers,[115] mechanical loading increases bond dissociation rates compared to the mechanical stress-free case, as was first emphasized by Bell,[116] in far from equilibrium situations. This complicates the use of AFM–SMFS for complex molecular architectures; however, it also presents opportunities to study well-defined systems for new perspectives, as important parameters of the potential energy landscape along the unbinding reaction coordinate can be determined from loading-rate dependences.[117] For stretching of covalent chains prior to rupture, one needs to consider the rate of chain-segment fluctuation (between the tip and the substrate) and the bond-loading rate of the AFM experiment. If the bond-loading rate

(chain-stretching rate) is much slower than the chain fluctuations, the macromolecule is in quasi-equilibrium during stretch; that is, no loading-rate dependence is anticipated. However, kinetic aspects of the internal conformational transitions during chain stretch may give rise to a loading-rate dependence, in particular when the experimental timescale becomes comparable to the molecular kinetics (single-chain viscoelasticity, plasticity, i.e., energy dissipation). In equilibrium, force curves (loading and unloading) should be fully reversible with no "snapping" of the cantilever upon bond separation. However, when single chains are stretched (loaded) and exhibit conformational transformations (e.g. for polymers with glycan rings "unclicked"—shorter—and "clicked"—longer—states) a loading-rate dependence can occur.[118]

An elastically coupled two-level model was proposed by Gaub et al.[119] to account for such loading-rate dependences. The model was capable of explaining the single-chain viscoelastic behavior (force vs extension) of very different biopolymers, and of modular polymers. Later, Hanke and Kreuzer[120] modified and generalized this treatment in the so-called "continuous two-state model", whereby conformational transitions in single molecules were modeled with a complete energy landscape.

As for an ideally elastic chain, loading and unloading force curves should overlap. One should check experimentally whether this condition is fulfilled, that is, whether no energy dissipation has taken place during single-molecule stretching.

2.2. Picking Up and Placing Single Chains

2.2.1. Picking Up Individual Macromolecules

As was mentioned in Section 2.1, stretching of a single polymer chain in an SMFS experiment implies it is anchored between a solid surface (i.e. the substrate) and the AFM tip, through both chemical and/or physical binding (i.e. physically adsorbed to both substrate and tip, chemically grafted to the substrate and physically to the tip, chemically grafted to the tip and physically to the substrate, or chemically grafted to both substrate and tip). Provided that a physical pickup with the AFM tip (adsorption) is utilized, and the polymer molecules can be physically adsorbed or chemically grafted to the substrate, it is important that the surfaces expose individual macromolecules with large intermolecular spacing. For physical adsorption of the polymer onto the substrate, such conditions can be achieved by preparing the surfaces from very dilute solutions and applying several rinsing steps after the incubation period. The optimal concentration of the polymer solution for sample preparation varies for different polymer systems.[87] Physical adsorption is generally used when the interaction between the macromolecules and the substrate is strong enough. This is the case for polysaccharides on glass or Si.[69–71]

For macromolecules chemically grafted to the substrate, surfaces can be prepared by exposure to a two-component solution consisting of the end-modified polymer chain and an end-modified inert short molecule (e.g. 11-mercapto-1-dodecanol and octadecanethiol, commonly used for gold substrates).[92] Compounds of *n*-alkanethiol are well-known to spontaneously form on Au surfaces a chemically and mechanically stable, highly ordered, self-assembled monolayer (SAM) in which the molecules are covalently attached to the surface through a gold–thiolate bond. The ratio of polymer and inert molecules as well as the incubation conditions may be varied to produce isolated, well-separated polymer chains. Zou et al.[121] developed a generic strategy to chemically graft isolated chains to gold surfaces. The method consisted in grafting ethylene sulfide-functionalized polymer chains into the defects of preformed SAMs of various ω-mercaptoalanols, from very dilute solutions (ca. 8×10^{-6} M). The defects in the SAMs were created by in situ exposure to toluene, and the end-functionalized polymer chains were inserted into these defects and covalently bonded to the substrate. The gold–thiol chemistry is effective for grafting macromolecules onto Au substrates, and silanization is another method commonly used for grafting single molecules onto glass or Si surfaces.[59,79,87,122] In addition to these "grafting to" methodologies, macromolecules can also be chemically bound to a surface via the "grafted from" technique, that is, by radical polymerization from immobilized initiators,[68] in which the grafting density is governed by controlling the initiator concentration on the surface, or by electrografting,[123,124] which mainly produces polymer brush surfaces with a moderate grafting density.

A strategy different from picking up the polymer chains bound to a substrate consists of tethering the polymer chains to the AFM tip, which can be accomplished by modifying the polymer with specific chemical species that can be grafted to the tip, for example, thiol groups to react with gold-coated tips.[58,125,126] Moreover, the tip's surface can be activated by chemical grafting of thiol-based compounds[63,65,66] on gold-coated tips, or by silanization[59,63,122,127] of Si_3N_4 tips, to react with a variety of chemical compounds, followed by the anchoring of various macromolecules. A very useful standard approach regarding Si or Si_3N_4 tip functionalization by macromolecules was developed by Hinterdorfer et al. using ethanolamine.[128] Their method involves three steps: 1) generation of amino groups at the tip surface; 2) attachment of a heterobifunctional polyethylene glycol (PEG) chain with an amino-reactive end; and finally 3) linking of the probe molecule to the functionalized end of the PEG chain.

An alternative approach for modifying AFM tips is the electrografting method proposed by the group of Duwez,[94,129] in which the polymer is chemically grafted to the surface of the tip by electropolymerization. Immobilization of the polymer chains on the tip may be more advantageous, to guarantee a dilute polymer system by controlling the density of chains attached to the tip. Besides, the obstacle of locating a single chain on the surface is avoided, thus leading to an increase in the frequency of stretching (pickup) events. This approach has been extensively used to study adsorption/desorption behavior on diverse surfaces for various polyelectrolytes grafted to an AFM tip.[63,65–67] Moreover, covalent binding of the polymer chain to both surface and tip simultaneously is a means to ensure that the entire length of the macromolecule undergoes stretching, and the method can be used to estimate the poly-

mer length.[126] This strategy is mainly used to determine rupture forces of covalent bonds, and allows the application of repeated stretching cycles on a single chain, which avoids rapid desorption or sliding of the polymer from the tip.[58,130,131]

2.2.2. Delivering Individual Macromolecules

Manipulating and delivering single macromolecules in a precise, controlled manner to a specific target is still a significant nanotechnological challenge. Recently, Duwez et al. portrayed the use of AFM for delivering and immobilizing individual molecules, one at a time, on a surface.[129] This approach consists in the modification of an AFM tip by electrografting. The reactive polymer molecules, attached at one end to the tip, are brought into contact with a silicon substrate modified with complementary moieties to which they become linked through a chemical reaction. The subsequent retraction of the AFM tip from the surface gives rise to a mechanical force that causes the weakest bond to break, that is, the one between the polymer and the tip. This process transfers the polymer molecule to the substrate where it can be modified by further chemical reactions. This molecule-by-molecule delivery process is shown in Figure 3, and in this case, gold-coated AFM tips were modified by electrografting of poly-*N*-succinimidyl acrylate (PNSA).

Electroinitiated polymerization is a convenient way of fabricating polymer brushes with a moderate grafting density.[123,124] Silicon substrates have been modified by grafting them with aminopropyltrimethoxysilane, and when bringing the tip and surface into contact at room temperature, the activated ester groups of the polymer readily react with the amino derivatives. The amide bonds covalently link the polymer to the substrate, and upon subsequent retraction of the tip, single chains are stretched until the breaking of a bond. As the Au(tip)–C-(polymer) bond is the weakest link in the system, it is considered the most likely candidate to break (the average value for the rupture force was observed at 1.1 ± 0.15 nN), and upon cleavage, the polymer chain remained covalently attached to the surface. Provided that the bond anchoring the molecule to the tip is weaker than the one to be established with the surface, this approach can be extended to various kinds of platforms. This method thus provides a tool that operates at the ultimate limits for fabrication of organic surfaces, that is, with single molecules.

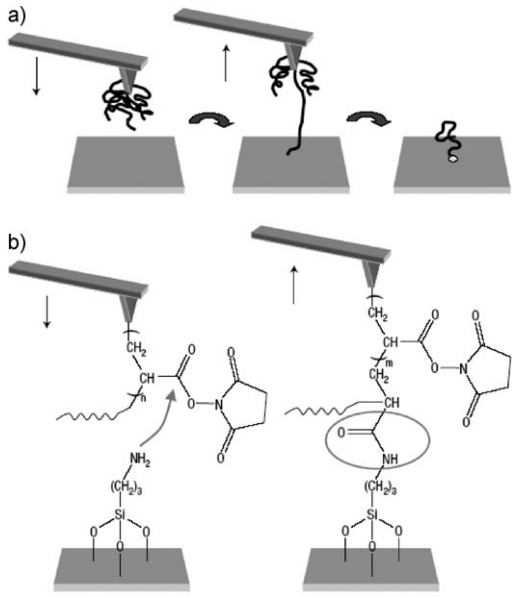

Figure 3. The molecule-by-molecule delivery process. a) Reactive polymer molecules attached to the AFM tip are brought into contact with a substrate to which they can become linked by a chemical reaction. When the tip is pulled away from the surface, the resulting mechanical force causes the bond between the tip and the molecule to break. b) During the tip–substrate contact, a chemical reaction occurs between the activated esters of the PNSA chain grafted to the tip and the amino groups of the substrate. This forms an amide bond, which covalently links the chain to the substrate. Reprinted by permission from Macmillan Publishers Ltd: Nature Nanotechnology,[129] copyright 2006.

3. Elasticity of Polymer Chains

The force–extension data recorded during stretching experiments are usually compared with the predictions of single-chain elasticity models derived from statistical mechanics. When a single polymer chain is stretched, two kinds of restoring forces occur. If a single chain adopts a random-coil conformation, Brownian molecular motion causes a permanent fluctuation of the molecule. Extension of the molecule leads to a reduction in the number of possible conformations, which causes a loss of conformational entropy. Hence, *entropic* forces dominate at short extensions (low stretching forces). Large elongations relative to the chain contour length between the tip and the substrate, on the other hand, lead to stresses in the molecular backbone. Bonds become stretched and deformed in the pulling direction, and the corresponding *enthalpic* elasticity is recorded in addition to the entropic forces. To describe the entropic elasticity of a polymer chain, two statistical mechanical models are mainly utilized, that is, the freely jointed chain (FJC)[38,132] and the wormlike chain (WLC)[133–137] models. Table 2 summarizes the most commonly used force (F)–extension (z) interpolation formulas for these models.

The FJC model treats a polymer chain as a number N of rigid Kuhn segments with lengths of l_k (Kuhn's segment length), connected through flexible joints without any long-range interactions. For low forces (small stretching), this model has been reported to provide a reasonable description of the stretching behavior of certain individual chains, such as DNA,[12] poly(methacrylic acid) (PMAA),[58,92] and polydimethylsiloxane (PDMS).[141]

The FJC model supposes each segment to have a fixed length (l_k), which indicates a fully elongated chain when the extension z equals the value $N \cdot l_k$. Consequently, if the chain was infinitely strong, the tension F would become infinite (see equation FJC in Table 2). This equation is thus a good approximation for small elongations (small applied forces) of the molecule.[132]

To cover the whole force range, a generic approach that takes into account the deformation of bonds and bond angles was developed, and is known as the modified or extended FJC (m-FJC or FJC$^+$) model.[138] This model extension considers the

Table 2. Elasticity models describing the force–extension relationship for single polymer chains.

Model	Force–distance expression	Fitting parameters
Freely jointed chain (FJC)[38]	$z(F) = L_c\left[\coth\left(\frac{Fl_k}{k_BT}\right) - \frac{k_BT}{Fl_k}\right]$	l_k, L_c
Wormlike chain (WLC) (Marko–Siggia)[136, 137]	$F(z) = \frac{k_BT}{l_p}\left[\frac{1}{4}\left(1-\frac{z}{L_c}\right)^{-2} + \frac{z}{L_c} - \frac{1}{4}\right]$	l_p, L_c
Extended FJC (FJC$^+$ or m-FJC)[138]	$z(F) = L_c\left[\coth\left(\frac{Fl_k}{k_BT}\right) - \frac{k_BT}{Fl_k}\right]\left(1+\frac{F}{K_sl_k}\right)$	l_k, L_c, K_s
Odijk WLC[139]	$z(F) = L_c\left[1 - \frac{1}{2}\left(\frac{k_BT}{Fl_p}\right)^{1/2} + \frac{F}{K}\right]$	l_p, L_c, K
Modified Marko–Siggia WLC (WLC$^+$)[44]	$F(z) = \frac{k_BT}{l_p}\left[\frac{1}{4}\left(1-\frac{z}{L_c}+\frac{F}{K_0}\right)^{-2} + \frac{z}{L_c} - \frac{F}{K_0} - \frac{1}{4}\right]$	l_p, L_c, K_0
Hooke-spring-modified WLC[140]	$F(z) = \frac{k_BT}{l_p}\left[\frac{1}{4}\left(1-\frac{z}{L_c}\right)^{-2} + \frac{z}{L_c} - \frac{1}{4}\right] + K'z$	l_p, L_c, K'

F: force; z: extension; k_B: Boltzmann's constant; T: temperature; L_c: contour length; l_k: Kuhn segment length; l_p: persistence length; K_s, K, K_0, K': elasticity parameters.

molecule as n identical elastic springs in series, and uses the segment elasticity K_s to describe each segment. The m-FJC model has been successfully used on a variety of synthetic polymers, such as polystyrene (PS),[142] poly(vinyl alcohol) (PVA),[49] poly(acrylic acid) (PAA),[143] PEG,[50] poly(*N*-isopropylacrylamide) (PNIPAM),[144] polyacrylamide (PAAM),[144] polydimethylacrylamide (PDMA),[56] polydiethylacrylamide (PDEA),[56] poly(2-acrylamido-2-methylpropanesulfonic acid) (PAMPS),[64] poly(ferrocenyldimethylsilane) (PFDMS),[121, 145–147] dendronized polymers,[148, 149] and poly(*N*-vinyl-2-pyrrolidone) (PVP),[52] as well as many polysaccharides, including dextran,[69, 70] amylose,[70] cellulose,[53, 70] carrageenan,[54, 74] curdlan,[150] and carboxymethylcellulose (CMC).[151] The fitting parameters and typical "pull-off" force values for the stretching behavior of synthetic polymers and polysaccharides under specific solvent conditions, as described by FJC models and reported in the literature, are displayed in Tables 3 and 4.

As opposed to the FJC model, the WLC model describes a polymer chain as a homogeneous string with a constant bending elasticity, and treats the molecule as a continuous entity with persistence length l_p. This parameter was introduced by Kratky and Porod[133, 134] as a direct measure of the average local conformation for a linear polymer chain. The persistence length reflects the sum of the average projections of all chain segments in a specific direction described by a given segment. Below this length the polymer is considered to be linear. The most commonly used expression for the WLC model is the interpolation formula of Marko and Siggia,[137] shown in Table 2. The WLC model has been effectively used to reproduce the force–extension behavior for short extensions of many biopolymers, such as DNA,[2, 9, 38, 137] proteins,[9, 89, 155] and certain synthetic polymers, for example, PDMS,[141, 156] PMAA,[58] block copolymers like polystyrene-*b*-poly(2-vinylpiridine) (PS-*b*-P2VP)[93] and poly(methyl methacrylate)-*b*-poly(4-vinylpiridine) (PMMA-*b*-P4VP),[157] poly(vinyl acetate) (PVAc),[51] PS,[126, 158] and PNIPAM.[159]

Although this approach takes into account both entropic and enthalpic contributions, the extension is limited by the contour length of the polymer (L_c), and the model fails for macromolecules under conditions of high stress. To broaden the range of applicability of the WLC model, the extended WLC models by Odijk[139] (Odijk WLC) and Wang[44] (modified Marko–Siggia) include a stretching term that is appropriate for intrinsic enthalpic contributions. In these equations (see Table 2), the parameters K and K_0 denote the specific stiffness of the polymer chain. In his work, Odijk[139] tackled the question of how the deformational behavior of the chain changes from entropy-dominated to elasticity-dominated as the level of stress exerted on it is increased. Odijk proposed a simple equation and was able to predict the onset of the deviations from the purely entropic behavior that Smith et al.[38] had observed for DNA stretching. The approach of Wang[44] also proved to fit reasonably well with experimental data for DNA elasticity over the range of applied forces up to 20 pN. The Marko–Siggia WLC, on the other hand, was found only to fit the experimental results in the low-force regime (<5 pN). The group of Evans[140] has also applied a simple modification to the WLC model, by introducing a linear spring term ($K'\cdot z$) (Hooke spring model) to represent the enthalpic contributions, so that [Eq. (6)]:

$$F(z) = \frac{k_BT}{l_p}\left[\frac{1}{4}\left(1-\frac{z}{L_c}\right)^{-2} + \frac{z}{L_c} - \frac{1}{4}\right] + K'z. \quad (6)$$

With this model it is possible to mimic the elastic properties of the nonglobular part of titin (PEVK) to a better degree than with the unmodified WLC model. The approach takes into consideration that the enthalpic properties contribute to the elastic properties of the chain, and uses a simple, classical expression with the advantage of approximating the polynomial form to the first-order term through Taylor expansion. This enables a direct evaluation of the spring term, in contrast to the nonlinear form used by Odijk[139] and Wang[44] (F/K; see Table 2). The modified Marko–Siggia WLC model has in some cases been used to describe the elasticity behavior of various polysaccharide macromolecules, such as hyaluronan (HA), methyl cellulose, and chitosan, as well as some connective tissue glycans.[160]

The Marko–Siggia interpolation formula has the property of reducing to the exact solution as either $z\rightarrow 0$ or $z\rightarrow L_c$. However, in between these values it reproduces the general behavior of the exact solution but may differ as much as 10% for $z/L_c \approx 0.5$,[136] and sometimes fails to describe the force–extension

Table 3. Overview of fitting parameters for the stretching behavior of synthetic polymers under specific solvent conditions, as described by FJC models. Reported contact rupture forces are also shown. These values correspond to breaking the weakest link, though the type and nature of the link is not specified. For comparison, according to Gaub et al.,[122] the strength of a covalent bond varies in the range of ≈2.8 nN (Si–C), ≈3.35 nN (Si–O), ≈4.1 nN (C–C) and (C–N), and ≈4.3 nN (C–O), whereas Au–Au rupture takes place at ≈1.5 nN.[152] The label p indicates physical adsorption to substrate and tip, cs, chemical binding to the substrate, and cst, chemical binding to both substrate and tip.

Synthetic polymers		Solvent conditions	Kuhn length l_k [nm]	Segment elasticity K_s [N m^{-1}]	Contact rupture forces [pN]	Model
Polystyrene (PS)[142]	p	toluene	1.22	2.1	200–250	m-FJC
Polystyrene (PS)[93]	p	10 mM sodium acetate buffer	0.37 ± 0.64	–		FJC
Polystyrene (PS)[147]	p	isopropanol	0.40 ± 0.03	18 ± 3		m-FJC
Poly(*N*-vinyl-2-pyrrolidone) (PVP)[52]	p	ethanol or THF	0.31	123		m-FJC
Poly(*N*-vinyl-2-pyrrolidone) (PVP)[93]	p	10 mM sodium acetate buffer	0.58 ± 0.28	–		FJC
PS-*b*-PVP[93]	p	10 mM sodium acetate buffer	0.36 ± 0.27	–		FJC
Poly(vinyl alcohol) (PVA)[49]	p	0.2 M NaCl (aq)	0.62	17	300–400	m-FJC
Poly(acrylic acid) (PAA)[143]	p	10^{-3} M KNO_3 (aq)	0.64	13	100–1800	m-FJC
Polyethylene glycol (PEG)[50]	cs	hexadexane	0.7	150	≈300	m-FJC
Poly(methacrylic acid) (PMAA)[92]	cs	water	0.33 ± 0.05	–	190 ± 110	FJC
Poly(methacrylic acid) (PMAA)[58]	cst	water		118	≈2200	m-FJC
Poly(*N*-isopropylacrylamide) (PNIPAM)[144]	p	water	0.70 ± 0.05	25 ± 2	500–1000	m-FJC
Poly(*N*-isopropylacrylamide) (PNIPAM)[144]	p	8 M urea (aq)	0.78 ± 0.06	40 ± 5	500–1000	m-FJC
Polyacrylamide (PAAM)[144]	p	8 M urea (aq)	0.60 ± 0.05	20 ± 3	750–1300	m-FJC
Polydimethylacrylamide (PDMA)[56]	p	NaOH (aq) pH 9	1.3 ± 0.1	12 ± 1	500–1500	m-FJC
Polydimethylacrylamide (PDMA)[56]	p	2 M urea (aq)	1.5 ± 0.1	16 ± 1		m-FJC
Polydimethylacrylamide (PDMA)[56]	p	8 M urea (aq)	2.8 ± 0.2	28 ± 1		m-FJC
Polydiethylacrylamide (PDEA)[56]	p	NaOH (aq) pH 9	1.6 ± 0.1	17 ± 1		m-FJC
Polydiethylacrylamide (PDEA)[56]	p	2 M urea (aq)	2.0 ± 0.1	21 ± 1		m-FJC
Polydiethylacrylamide (PDEA)[56]	p	8 M urea (aq)	2.8 ± 0.2	28 ± 1		m-FJC
Poly[(diethylamino)ethyl methacrylate] (PDEAMA)[153]	cs	pH 10 buffer	0.37 ± 0.19	–		FJC
Poly[(diethylamino)ethyl methacrylate] (PDEAMA)[153]	cs	pH 4 buffer	0.19 ± 0.12	–		FJC
Poly(2-acrylamido-2-methylpropanesulfonic acid) (PAMPS)[64]	p	water	0.5	110	750–1600	m-FJC
PAMPS-*co*-crown[64]	p	water	1.0	12		m-FJC
Poly(ferrocenyldimethylsilane) (PFDMS)[145]	p	THF	0.41 ± 0.01	53 ± 1	400–1300	m-FJC
Poly(ferrocenyldimethylsilane) (PFDMS)[121]	cs	isopropanol	0.33 ± 0.05	32 ± 5	≈600	m-FJC
Poly(ferrocenyldimethylsilane) (PFDMS)[146, 147]	cs	0.1 M $NaClO_4$ (aq)	0.38 ± 0.03	30 ± 4	200–250	m-FJC
Poly(ferrocenyldimethylsilane) (PFDMS)[147]	p	isopropanol	0.37 ± 0.04	31 ± 4	170–470	m-FJC
Poly(ferrocenyldimethylsilane) (PFDMS)[147]	p	0.1 M $NaClO_4$ (aq)	0.39 ± 0.05	35 ± 6	450–700	m-FJC
Oxidized (chemically) poly(ferrocenyldimethylsilane) (o-PFDMS)[145]	p	THF	0.46 ± 0.01	115 ± 1		m-FJC
Oxidized (electrochemically) poly(ferrocenyldimethylsilane) (o-PFDMS)[146]	cs	0.1 M $NaClO_4$ (aq)	0.65 ± 0.05	45 ± 8	125–250	m-FJC
Oxidized (electrochemically) poly(ferrocenyldimethylsilane) (o-PFDMS)[147]	p	0.1 M $NaClO_4$ (aq)	0.63 ± 0.04	39 ± 6	100–400	m-FJC
Poly(ferrocenylmethylphenylsilane) (PFMPS)[145]	p	THF	0.36 ± 0.01	61 ± 1	700–1300	m-FJC
Oxidized (chemically) poly(ferrocenylmethylphenylsilane) (o-PFMPS)[145]	p	THF	0.40 ± 0.01	500 ± 1		m-FJC
PFDMS-*b*-PS[147]	p	isopropanol	0.39 ± 0.05	23 ± 5		m-FJC
Dendronized poly(*p*-phenylene) (hydrophobic) (hPPP)[148]	p	THF	0.33 ± 0.01	80 ± 1	500–2000	m-FJC
Dendronized poly(*p*-phenylene) (hydrophobic) (hPPP)[148]	p	CH_2Cl_2	≈0.33	≈80		m-FJC
Dendronized poly(*p*-phenylene) (amphiphilic) (aPPP)[148]	p	THF	0.42 ± 0.01	84 ± 1	500–1500	m-FJC
Dendronized poly(*p*-phenylene) (amphiphilic) (aPPP)[148]	p	CH_2Cl_2	0.40 ± 0.01	80 ± 1		m-FJC
Dendronized copolymer G1MA-*g*-BA[149]	p	THF	0.34 ± 0.01	53 ± 1	700–1700	m-FJC
Dendronized copolymer G1MA-*g*-BA[149]	p	$CHCl_3$	0.34 ± 0.01	109 ± 1		m-FJC
Dendronized copolymer G2MA-*g*-BA[149]	p	THF	0.31 ± 0.01	85 ± 1		m-FJC
Dendronized copolymer G2MA-*g*-BA[149]	p	$CHCl_3$	0.31 ± 0.01	85 ± 1		m-FJC
Dendronized copolymer G3MA-*g*-BA[149]	p	THF	0.31 ± 0.01	85 ± 1		m-FJC
Dendronized copolymer G3MA-*g*-BA[149]	p	$CHCl_3$	0.31 ± 0.01	85 ± 1		m-FJC
Poly(2-hydroxyethyl methacrylate-*g*-ethylene glycol) (poly(-HEMA-*g*-EG))[154]	cs	PBS buffer	0.52 ± 0.09	10.5 ± 3.3	160 ± 130	m-FJC
Poly(2-hydroxyethyl methacrylate-*g*-ethylene glycol) (poly(-HEMA-*g*-EG))[154]	cs	water	1.03 ± 0.01	4.2 ± 0.5	120 ± 110	m-FJC

Table 4. Overview of fitting parameters for the stretching behavior of polysaccharides under specific solvent conditions, as described by FJC models. (see Table 3 heading for conditions).

Polysaccharides		Solvent conditions	Kuhn length l_k [nm]	Segment elasticity K_s [N m^{-1}]	Contact rupture forces [pN]	Model
Hydrophobically modified ethyl hydroxyethylcellulose (HM-EHEC) below critical conc.[53]	p	water	1.60 ± 0.10	26.5 ± 1.6	800–1700	m-FJC
HM-EHEC above critical conc.[53]	p	water	1.10 ± 0.15	25.5 ± 1.5	670–1100	m-FJC
ι-Carrageenan[54,74]	p	water	1.3	42	1400–4500	m-FJC
κ-Carrageenan[74]	p	water	1.3	41 ± 1	1400–4500	m-FJC
λ-Carrageenan[74]	p	water	1.05 1.18	17 ± 1[a] 41 ± 1[b]	1000–3000	m-FJC
Curdlan[150]	p	0.5 M NaOH (aq)	1.40 ± 0.10	11 ± 1	700–2400	m-FJC
Dextran[69]	p	physiological buffer	0.60 ± 0.05	6.7 ± 1[a]		m-FJC
Dextran[70]	p	water	0.44	14.6 ± 2.7[a]		m-FJC
Dextran[82]	p	PBS buffer	0.44 0.57	11.5[a] 90.2[b]		m-FJC
Periodate-oxidized dextran[70]	p	water	0.20 ± 0.026	34.2 ± 8.3		m-FJC
Amylose[70]	p	water	0.45	5.6 ± 0.8[a]		m-FJC
Periodate-oxidized amylose[70]	p	water	0.18 ± 0.025	34.0 ± 7.3		m-FJC
Pullulan[70]	p	water	0.45	10.2 ± 0.93[a]		m-FJC
Periodate-oxidized pullulan[70]	p	water	0.20 ± 0.015	47.8 ± 5.0		m-FJC
Pectin[72]	p	PBS buffer	1.81	17.0[a] 24.0[b] 83.0[c]		m-FJC
Carboxymethylamylose (CM-amylose)[71]	p	PBS buffer	0.54	11[a] 28[b]		m-FJC
Carboxymethylcellulose (CMC)[71]	p	PBS buffer	≈4	≈50		m-FJC
Xanthan (denatured)[86]	p	water		50 ± 5		m-FJC

[a] Before conformational transition. [b] After conformational transition. [c] After second conformational transition.

behavior in the full range of forces. Many authors have encountered this inconsequence of the Marko–Siggia interpolation with the various force regimes. As has been reported by the group of Seitz,[59] the fitting parameters may depend considerably on the range of forces used for the fit, which suggests that the spring constant (defined as K_0/L_c) determined in such studies may not be a material constant but rather that it may function as a heuristic parameter that makes up for imperfections of the fitting model employed. Hugel et al.[59] observed a dependence of the fit parameters on the choice of the force range when using the modified Marko–Siggia expression to fit the experimental force–distance profiles of polyvinylamines. Recently, Cuenot et al.[124] reported a dependence of the persistence length (l_p) values with the force range used for the fitting with the WLC model for PNSA. The group of Gaub[130,131] used the extended Marko–Siggia formula to fit the elastic response of a polyazopeptide, by taking into account the validity of this approximation to the exact solution of the WLC model only for the low- and high-force regimes.

In an attempt to improve the fitting results, Croquette et al.[161] subtracted the Marko–Siggia interpolation formula from the exact numerical solution of the WLC model and expressed the residuals as a seventh-order polynomial providing all the correction terms. The interpolation formula proposed by Croquette et al. was successfully used by Hinterdorfer and co-workers[162] to fit the stretching response of single PEG chains in the entire force range. Moreover, this notion has been backed up by some recent theoretical investigations showing that a freely rotating chain (FRC) model exhibits a crossover from WLC behavior at small stretching forces to a regime dominated by a discrete nature of the chain at large forces.[163–168] Furthermore, certain modifications of the WLC models within the three-dimensional continuum mechanics framework have also been reported.[168]

Table 5 presents the fitting parameters and typical "pull-off" force values for synthetic polymers under specific solvent conditions, as described by WLC models and reported in the literature. Deviations of the force–extension behavior from these models usually reflect structural transitions that are subjected to further analysis and modeling, as is discussed in Section 4.1.

3.1. Fitting of Experimental Data to Theoretical Models

To compare the force–extension data recorded during the stretching experiments with the predictions of single-chain elasticity models derived from statistical mechanics, a fitting of the data with the various models must be carried out. Least-squares methods are often used to obtain the fitting parameters, and the most commonly used is the nonlinear, rapidly converging, regression method based on the Marquardt–Levenberg algorithm.[170]

This procedure is quite simple in the case where direct functions are used, that is, Marko–Siggia WLC or the Hooke-spring-modified WLC interpolation formulas (see Table 2). This is due

Table 5. Overview of fitting parameters for the stretching behavior of synthetic polymers under specific solvent conditions, as described by WLC models. Reported contact rupture forces are also shown. These values correspond to breaking the weakest link, although the type and nature of the link is not specified. For comparison, according to Gaub et al.,[122] the strength of a covalent bond varies in the range of ≈2.8 nN (Si–C), ≈3.35 nN (Si–O), ≈4.1 nN (C–C) and (C–N), and ≈4.3 nN (C–O), whereas Au–Au rupture takes place at ≈1.5 nN.[152] The label p indicates physical adsorption to substrate and tip, cs, chemical binding to the substrate, and cst, chemical binding to both substrate and tip.

Macromolecule		Solvent conditions	Persistence length l_p [nm]	Specific stiffness K [nN]	Contact rupture forces [pN]	Model
Polystyrene (PS)[93]	p	10 mM sodium acetate buffer	0.37 ± 2.11	–		WLC
Polystyrene (PS)[126]	cst	DMF	0.56	–	≈140	WLC
Polystyrene (PS)[169]	cst	cyclohexane	0.31 ± 0.01	–	200–500	WLC
Polystyrene (PS)[158]	cs		0.23 ± 0.10	–		WLC
Poly(*N*-vinyl-2-pyrrolidone) (PVP)[93]	p	10 mM sodium acetate buffer	0.40 ± 0.32	–		WLC
PS-*b*-PVP[93]	p	10 mM sodium acetate buffer	0.30 ± 0.26	–		WLC
Polydimethylsiloxane (PDMS)[156]	cs	25 mM NaCl (aq)	0.13	–	100–2000	WLC
Poly(vinyl acetate) (PVAc)[51]	p	3-heptanone	0.31	–		WLC
Poly(vinyl alcohol) (PVA)[51]	p	0.2 M NaCl (aq)	1.0	–	1030–1250	WLC
Poly(vinyl alcohol) (PVA)[51]	p	8 M urea (aq)	0.16	–		WLC
Polyvinylamine (10% hydrolysis)[59]	cs	5 mM NaCl (aq)	0.8 ± 0.16	5.1 ± 2.5		WLC^+
Polyazopeptide[130,131]	cst	DMSO	0.5	20		WLC^+
Poly(methacrylic acid) (PMAA)[92]	cs	water	0.28 ± 0.05	–	190 ± 110	WLC
Poly(ethylene glycol) (PEG)[162]	cst	PBS buffer	0.380 ± 0.002	1.561 ± 0.033		WLC^+
Poly(methyl methacrylate)-*b*-poly(4-vinylpyridine) (PMMA-*b*-P4VP)[157]	cs	toluene	0.3	–	550 ± 240	WLC
Poly(*N*-isopropylacrylamide) (PNIPAM)[159]	p	water	0.4	–	≈100	WLC
Poly(*N*-succinimidyl acrylate) (PNSA)[124]	cs	DMF	0.95	–		WLC
Poly(*N*-succinimidyl acrylate) (PNSA)[129]	cst	DMF	0.35		1100 ± 150	Odijk WLC

to the experimental data normally being in the form of force (F) as a function of extension (z). The fitting parameters (l_p and L_c for WLC, and also K' for the modified WLC) can thus be directly obtained. For the FJC, extended FJC, and Odijk WLC models, on the other hand, no expression of $F(z)$ is possible and the equations have the form of $z(F)$. Consequently, before applying the fitting algorithm, an inversion has to be carried out of the data to be fitted. Even for cases where this fitting procedure has been successfully applied (examples are cited in the previous section), special attention must sometimes be paid to the validity of the method used, especially for short polymeric chains, where the stretching event occurs in the low-extension regime. The dispersion of the experimental data, mainly for the independent variable (the force in this case), thus becomes displayed in the dependent coordinate (x axis). The spreading of the data is not constant along the whole force regime, but is higher at low forces (mainly the entropic region) and lower in the high-force part of the curve, where the force increases much more rapidly with small extension steps. This may prevent the Marquardt–Levenberg algorithm from being suitable in many cases, and it may be required to introduce weighting factors according to the error values.

Nonetheless, special attention has to be paid when considering the validity of these models, regardless of the length of the chain, to describe the force–extension behavior of the different polymeric systems. First, it should be taken into consideration that these statistical models assume a Gaussian behavior of the macromolecular chains, that is, at high extensions relative to the chain contour length between tip and substrate the models fail. Similar problems arise when the overall contour length of the polymer chain is short. Under these conditions the chain statistics cannot be assumed as Gaussian. Moreover, the larger the number of segments (N), the softer is the "spring". This correspondence is merely a reflection of the fact that, for a given elongation, each chain segment becomes less oriented for increasing number of N. In other words, short chains become highly orientated even at low strains and may cause an over-proportionate contribution to the tensile stress.[132]

3.2. Criteria for Single-Chain Detection

In an SMFS experiment, it is crucial to record the behavior of only one polymer molecule. As the probe's size is significantly larger than the size of the molecules, several chains are in some cases captured and handled at the same time. To minimize this problem, a number of strategies may be taken into account to limit the experimental conditions to single molecules, as well as to facilitate the identification of individual events in the resulting data. One of the main points to consider is the sample preparation. The various ways to prepare a sample in order for it to expose individual polymer chains that

can be picked up by the AFM tip, as well as single-chain placing strategies, were discussed in Section 2.2.

3.2.1. Individual Events in the Force–Extension Results

The appearance of only one force signal in the force profile during an SMFS experiment may be an indication that a single chain is being stretched, but this is not always the case. In the case in which only one end of the macromolecule (or none) is chemically bound to either the substrate or the AFM tip, the extension length of the chain will vary, as the chain is picked up at random. This is reflected in the different "contour lengths" observed for each individual experiment, and would likewise be observed if both ends of the chains were chemically grafted to both surface and tip, and the polymer chains had a large size distribution. However, if the resulting force–extension curves are normalized by their extension value at a certain common force value, the force-normalized extension curves can be plotted as a normalized single curve. An example of this is depicted in Figure 4. If single molecules are stretched, the normalized curves superimpose well, since the elastic properties scale linearly with the contour length.[69]

When employing one of the theoretical models summarized in Table 2 to describe the elastic behavior of single macromolecules, it becomes possible to fit the experimental force curves to the corresponding equation and to obtain the fitting parameters [i.e. the corresponding segment (or persistence) length and segment elasticity]. These parameters are intrinsic properties, independent of the contour length. Thus, when single molecules are stretched, the segment length and elasticity values should be identical within experimental error. It has been reported that fitting force curves corresponding to multiple chains in parallel may require very low, nonphysical, persistence length values, much lower even than the size of a monomer.[93,171] This issue requires thorough future investigation.

The linear scaling of the elastic properties with the contour length and the identical segment elasticities and segment lengths for all the pulling events corroborate the fact that individual chains are stretched and the deformation of a single chain under tension is being measured.

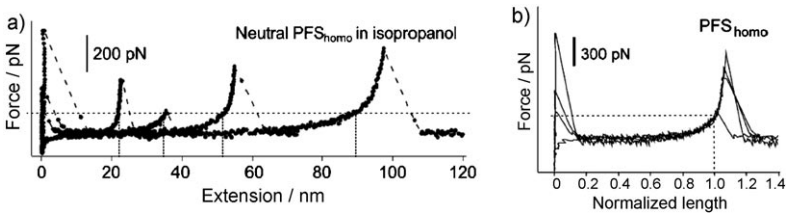

Figure 4. a) Force–extension traces of individual, neutral poly(ferrocenylsilane) homopolymer (PFS_{homo}) measured in isopropanol and b) superposition of force curves for PFS_{homo} normalized to a force value of 250 pN. The dotted line indicates the force chosen for normalization. Adapted from ref. [147] with permission from Elsevier.

4. SMFS and Conformational Transitions

This section demonstrates how SMFS allows the analysis of single macromolecule conformations, specifically that induced by the application of stress to the molecule, such as the force-induced conformational transitions in polysaccharides and the detection and rupture of secondary structures of macromolecules. SMFS also allows the characterization of various conformational states of polymer chains induced by external stimuli, and their application to building molecular machines.

4.1. Mechanically Induced Changes in Conformation

Many natural as well as synthetic macromolecular systems may undergo conformational transitions under externally applied forces. As mentioned previously, AFM-SMFS has become a powerful technique to detect and study these transitions at the single-chain level, by analyzing the elastic response of the macromolecule under certain environmental conditions.

4.1.1. Force-Induced Conformational Transitions in Polysaccharides

SMFS is a very useful technique to directly identify the linkage of pyranose rings in polysaccharides, as the stiffening of the chains at a certain force due to a conformational change (specific for each linkage type) is clearly evidenced in the force–extension data.

Rief et al.[69] were the first to identify a transition into a stiffer conformation when stretching dextran molecules, revealed as a plateau in the force–extension signal at 250–350 pN for carboxymethylated dextran, and at 700–850 pN for native dextran (see Figure 5). This transition had been predicted by molecular dynamics simulations and was ascribed to a purely elastic and reversible conformational change of the polysaccharide, due to rotation of an exocyclic bond. Marszalek et al.[70] observed the same plateau region in the force–extension response for dextran and amylose. In accordance with theoretical calculations, they identified it as a chair-to-boat conformational transition of the pyranose rings induced by the stretching force; a thermodynamically accessible conformation but normally less populated due to its high conformational energy. Independently, the groups of Gaub and Zhang[71] simultaneously reported on the chair-to-twisted-boat transition in α-(1,4)-linked polysaccharides. Contrarily, β-(1,4)-linked polysaccharides demonstrate a stiff and extended conformation, and consequently do not present this force-induced conformational transition, which is thus called a nanomechanical "fingerprint" of the α-(1,4)-linked glycans. Subsequently, these observations were expanded to include chair inversions for pectin molecules,[72] which consist in a resolved two-step

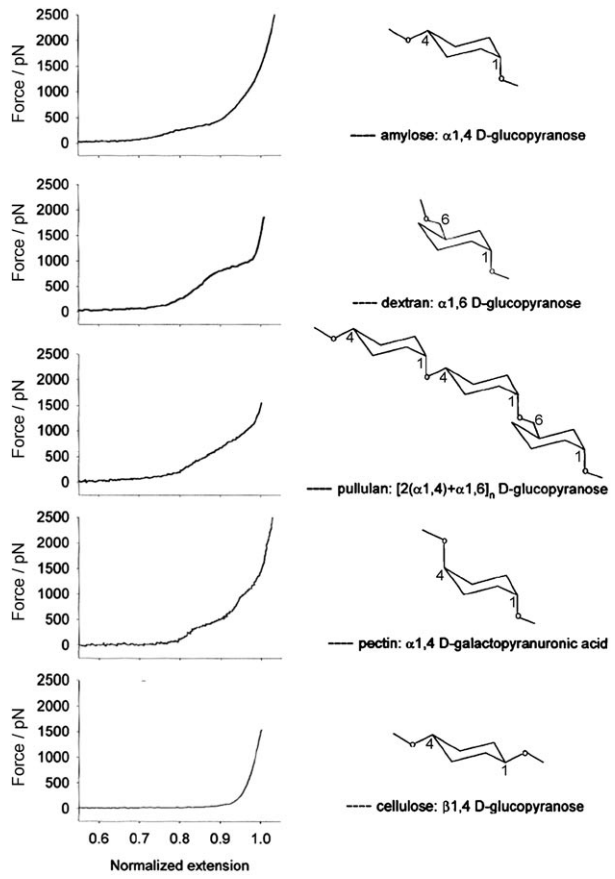

Figure 5. "Fingerprints" of elasticity for linear polysaccharides as obtained by AFM-SMFS. The simplified monomeric structure and type of glycosidic linkage in the polysaccharides are displayed on the right, and the corresponding force–extension curves (extensions normalized by the length of the molecules at equal forces) are displayed to the left. The deviations from pure entropic elasticity shown for all cases, with the exception of cellulose, are the "fingerprint" characteristics of monomers and linkages. Reprinted by permission from Macmillan Publishers Ltd: Nature Biotechnology,[73] copyright 2001.

conversion on the pyranose ring conformation from a chair to a boat and then to an inverted chair.

Marszalek and Fernandez[73] have published a brief yet complete overview of fingerprinting polysaccharides in an article that reports the use of AFM–SMFS for identifying individual polysaccharide molecules in solution. Figure 5 shows the "fingerprints" of elasticity for linear polysaccharides according to the type of glycosidic linkage. Similar conformational transitions have been observed during SMFS investigations of heparin,[83] a polysaccharide that plays a major role in defining the physical and chemical properties of the extracellular matrix. It is believed that it is under mechanical stress in vivo and that it undergoes physiologically significant force-driven conformations. According to theoretical predictions, the force-induced conformational transition of the pyranose ring will not occur if an oxygen bridge is introduced over this ring as a result of a spatial barrier.[172] The group of Zhang[74] experimentally demonstrated this prediction by monitoring the fingerprint of the chair-to-inverted-chair transition for carrageenan single chains by SMFS. At the same time, Marszalek et al.[75] introduced the use of force-ramp AFM (see Section 2.1.1) for the conformational transition analysis, which captures the ring transitions under conditions where the entropic elasticity of the molecule is separated from its conformational transitions, thus enabling a quantitative analysis of the data with a simple two-state model.

In contrast to the (1,4)-linkage, which transmits the stretching forces to the pyranose ring along its axis of symmetry, other linkages, such as (1,6), attach the force vector to the sides of the ring at various positions and angles. Recently, Lee et al.[77,85] reported on force-induced conformational transitions for α- and β-(1,6)-linked polysaccharides. Even when the force–extension curves present a plateau similar to the one observed for (1,4)-linked polysaccharides, the conformational transitions of β-(1,6)-linked pustulan (between 100 and 700 pN) correspond to a rotation of the exocyclic group on the glucopyranose ring. Furthermore, the elasticity for α-(1,6)-linked dextran is dominated by conformational transitions involving both rotations around the exocyclic C_5–C_6 bond and chair–boat transitions, which show a plateau at about 700 pN. Walther et al.[82] demonstrated the use of variance analysis to capture dynamic molecular conformations of dextran molecules stretched by AFM, which supports the chair–boat transition. The analysis of the variance of the molecule's fluctuations verifies the equilibrium throughout the force–extension curve, and validates the analysis of the variance in the transition region, thus revealing an intermediate conformation between the chair and the boat on the sub-Angstrom scale.

These results demonstrate how the application of the AFM–SMFS technique has been expanded to effectively identify carbohydrate isomers and mechanically manipulate single pyranose rings.[81] The analysis of conformational transitions in polysaccharides has been reviewed by the groups of Zhang[87] and Marszalek.[79]

4.1.2. Specific Secondary Structures in Synthetic Polymers and Polysaccharides, Detected and Ruptured by SMFS

SMFS is also a very useful technique for detecting secondary structures of various polymer systems. As a result of the force that is applied during the chain extension breaking the structure, the transition can be detected in the elastic response of the molecule.

In 1999, the group of Gaub[50] reported on marked deviations in the transition region from entropic to enthalpic elasticity for SMFS experiments on PEG in water. These deviations indicated the deformation of a secondary structure (referred to as "superstructure") within the polymer, stabilized by water binding. At forces around a few piconewtons, entropic restoring forces explained the elastic response of PEG in water, whereas at hundreds of piconewtons, the elasticity was purely enthalpic and could be explained by bond distortion. However, between the two extremes, water molecules were found to form fluctuating intramolecular bridges, thus shortening the net polymer length and resisting further extension. This transition was found to be reversible. Similar observations were previously reported for the polysaccharide xanthan.[86,173] A pla-

teau in the force–extension curves was present in the stretching response of native xanthan molecules but not in the denatured ones. This was an irreversible transition, ascribed to an ordered, helical, secondary structure stabilized by noncovalent interactions, such as hydrogen bonds and electrostatic interactions.

A similar kind of suprastructure was discovered by SMFS for PAAM[144] and PVP.[52] Their elastic response showed a deviation from the m-FJC model at the middle force regime, probably due to the formation of intramolecular H bonds in water as well as H bonds between the solvent and the polymer. Several studies on amylose[55,78,174] revealed that the polysaccharide may form inter-residue H bonds under various solvent conditions. As described in Section 4.1.1, the pyranose rings in amylose can undergo a chair–boat conformational transition upon stretching. The presence of an intermolecular H-bonding structure under certain solvent conditions can in some cases be evidenced as a plateau in the force–extension signals before the chair–boat transition,[55] as the displacement of the plateau to higher forces in other cases,[78] or even by its elimination.[174]

Apart from exposing secondary structures of individual molecules, SMFS has also revealed the force-induced breaking of multiple-stranded structures. Examples include PVA,[51] which assumes a multiple-stranded helical structure stabilized by hydrogen bonding in water, and undergoes a conformational transition to an overstretched state upon stretching, and also the polysaccharide curdlan,[150] where SMFS is able to recognize triple and double helices in a force-induced transition from a helical structure to a random-coil structure.

A recent paper from Zhang and Marszalek[80] summarizes the use of SMFS for the exploration of ordered secondary structures of individual polysaccharide chains and their multistrand complexes.

4.2. Conformational Changes Induced by External Stimuli

Stimuli-responsive polymers are defined as polymers that undergo relatively large and abrupt chemical or physical changes in response to small changes in the environmental conditions.[175] These polymers recognize a stimulus as a signal and subsequently alter their chain conformation as a direct response. The stimuli, which can be either physical (e.g. temperature, electric or magnetic fields, mechanical stress) or chemical (e.g. pH, ionic strength, chemical agents), induce changes in interactions between segments of the polymer chains, or between polymer chains and solvent molecules. The response of a polymer system to stimuli is a common process for biopolymers in living organisms. Synthetic polymers designed to mimic these biopolymers have been actively developed due to their industrial and scientific value.

AFM-SMFS has proven to be a very valuable tool for characterizing conformational changes in polymer chains. The combination of this tool and the great potential of stimuli-responsive polymers has opened a new area of research on artificial molecular motors at a single-molecule level, aimed at obtaining a fundamental understanding of the relevant molecular-scale processes and at realizing and exploiting the smallest man-made, artificial machinery.[130,131,146,147,153,176]

4.2.1. A Single-Molecule Optomechanical Cycle

The first demonstration of photomechanical energy conversion in an individual molecule was reported by the group of Gaub,[130,131] who showed the reversible, optical switching of individual molecules of a polymer containing azobenzene groups in the backbone, namely, a polyazopeptide. The group demonstrated how the contour length of the polymer was selectively lengthened or shortened by switching between *trans*- and *cis*-azo configurations when applying wavelengths of specific ultraviolet light (see below). Changes in contour length were reported, both at low forces and under external loads of up to 400 pN. It was demonstrated that the mechanical stability of the two azobenzene configurations is sufficient to operate the experiment in an optomechanical cycle, and thus to perform work at the molecular level.

Figure 6a shows a schematic diagram of the experimental setup and the change in the force–extension response of the optically excited and nonexcited molecules. The experiment starts with a relaxed polymer chain in an undefined, initially configurationally mixed state (black trace, $L = 86.5$ nm). By the application of five 420 nm pulses, the polymer was switched to the saturated *trans* state and lengthened by about 1.4 nm (dark grey). After five pulses at 365 nm, the same molecule was shortened by $\Delta L = 2.8$ nm (light grey). To obtain the contour lengths L of the stretched polymer molecules, the force–extension data are fitted with the extended WLC model. These results are shown on the right in Figure 6a. In the traces to the left, a single polyazopeptide strand was shortened against an

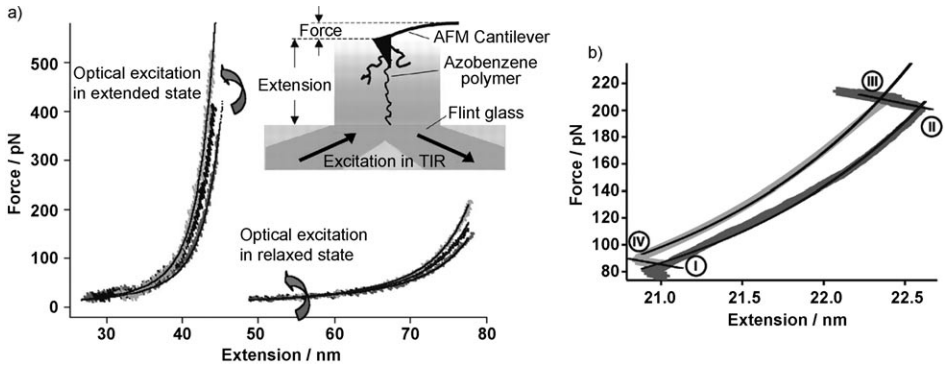

Figure 6. a) The traces to the right portray the force–extension of a single polyazopeptide. Traces to the left correspond to a single polyazopeptide strand being shortened against an external force. Inset: schematic of the experimental setup. TIR: total internal reflection. b) Experimental realization of the single-molecule operating cycle with polyazopeptides. Reprinted from ref. [131] with permission from AAAS.

external force. The strand was first driven into the *trans* state by five pulses at 420 nm, after which it was stretched to a force of about 350 pN (dark grey). The application of one pulse at 365 nm at a constant tip/sample separation results in a shortening of approximately 1.1 nm (black middle trace). Two further pulses resulted in an additional shortening by 0.8 nm (light grey trace). None of five additional pulses was found to result in any further shortening, and thus the polymer was assumed to be in the saturated *cis* state.

The closing of a cycle was carried out in the way portrayed in Figure 6b: an individual azopolymer was first optically lengthened (pulse application; I), and then mechanically expanded to a certain restoring force (II). The application of a new pulse contracted the polymer against the external force (III), and finally the force was again reduced (IV). The cycle was completed by the optical expansion of the molecule to its original state. As the mechanical work at the molecular level is a result of a macroscopic optical excitation, the real quantum efficiency of optomechanical switching for the cycle in the AFM setup is only on the order of 10^{-18}. However, the maximum efficiency of the optomechanical energy conversion at a molecular level was estimated to be about 10%.

4.2.2. Towards Redox-Driven Single-Chain Motors

Recently, the group of Vancso investigated various stimuli-responsive poly(ferrocenylsilane) (PFS) polymers as model systems for the realization of molecular motors powered by a redox process, in which the excitation can be more easily confined to a small number of macromolecules.[146,147] These polymers feature ferrocene units in the main chain bridged by substituted silanes,[177,178] which render the polymer chain electrochemically responsive (redox response). The complete and reversible oxidation (and reduction) of surface-confined PFS molecules in situ was carried out by applying an electrochemical potential in electrochemical AFM (EC–AFM). A decrease in entropic elasticity of PFS upon oxidation was obtained in the low-force regime. Preliminary studies on the elasticity of neutral[121] and ex situ chemically oxidized PFS[145] have been reported, but the latest studies[146,147] revealed that the elasticities could be reversibly controlled in situ by adjusting the applied potential in electrochemical SMFS experiments. The detected changes in elasticity of individual electrochemical-stimulus-responsive PFS chains are the basis for the demonstration of the principle of a single (macro)molecular motor.

As illustrated in Figure 7, when using a single polymer chain as a working substance, the mechanical work (output) of the cycle corresponds to the effectively converted electrochemical potential. One possible cycle to realize a molecular motor is defined by keeping the deflection of the cantilever constant in the SMFS experiment, that is, constant force, during the transition from the oxidized to the neutral state (and vice versa). The two branches of the cycle are determined by the elasticities of the polymer, which are well-described by the m-FJC model in the low-force range. Starting from a force of 20 pN (point 1 in Figure 7) under an applied constant external potential of +0.5 V, an individual, oxidized PFS polymer chain with a

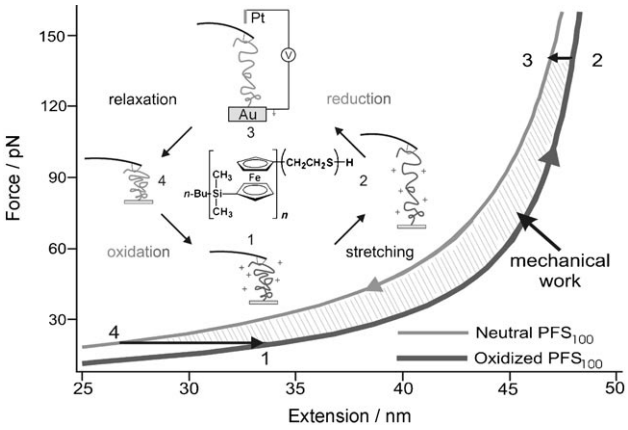

Figure 7. Force–extension curves of a single-molecule motor based on one PFS macromolecule driven by an electrochemical potential. The two curves are plotted based on the m-FJC function with l_k values of 0.38 nm (neutral PFS) and 0.65 nm (oxidized PFS), and $K_{segment}$ values of 30 nN nm^{-1} (neutral PFS) and 45 nN nm^{-1} (oxidized PFS), as observed experimentally. Inset: Schematic illustration of a single-molecule operating cycle with redox-active macromolecules. Adapted from ref. [146] with permission from Wiley-VCH.

50 nm contour length is pulled to a force of 140 pN (point 2). At a constant force of 140 pN, the PFS chain is reduced to its neutral state by controlling the external potential back to 0 V (point 3), thus giving rise to a change in the elasticity of the polymer chain. Subsequently, the force on the polymer is reduced back to 20 pN (point 4) and finally, the cycle is completed by applying an external potential of +0.5 V to completely oxidize the whole PFS chain. By periodically controlling the external potential, the corresponding oxidized and/or neutral PFS chains can be created to realize the operating cycle. The mechanical work performed by the PFS chain of approximately 3.4×10^{-19} J was calculated as the integrated area of the cycle shown in Figure 7. An efficiency of about 5% was estimated based on the experimental data. The closed electromechanical cycle was realized and will be reported in a separate paper.

5. Summary and Outlook

Manipulation techniques for single macromolecules are in continuous development due to their significant contributions towards the comprehension of physical/chemical processes, the structural details of biomacromolecules, and their role in natural biological functions, as well as towards figuring out the structure and conformation of synthetic polymers. AFM stands out as a great tool with an increasing potential for handling polymers at a single-chain level. The present review has exposed selected nanomechanical experiments on individual flexible macromolecules, and directed the attention to the use of AFM–SMFS for evaluating the elasticity of single macromolecules and understanding their conformational behavior along with the processes associated with it. As regards the experiments, there is room for further improvement of instrument stability, piezo creep, feedback loop operation, and environmental control to enhance data quality. Complementary theoretical analysis of the elastic behavior of polymer chains con-

tributes to the analysis and interpretation of the empirical evidence provided by this technique. Specifically, simulation, modeling, and a thorough revisiting of the various chain elasticity models (fitting) would contribute to having reliable quantitative data to characterize single chains. Yet, we believe that a higher level of cooperation between these two fields is essential to fully exploit the potential of this methodology. SMFS is in rapid expansion in combination with other detection/characterization techniques (e.g. single-molecule imaging) and will soon encompass the study of further complicated systems.

Acknowledgements

The authors gratefully acknowledge the European Commission (IIF Marie Curie fellowship, MIF1-CT-2004-008919) and the MESA+ Institute for Nanotechnology (University of Twente) for financial support.

Keywords: atomic force microscopy · conformation · force spectroscopy · polymers · single-molecule studies

[1] G. J. Fleer, M. A. Cohen Stuart, J. M. H. M. Scheutjens, T. Cosgrove, *Polymers at Interfaces*, Chapman & Hall, London, **1993**.
[2] P. A. Wiggins, P. C. Nelson, *Phys. Rev. E* **2006**, *73*, 031906.
[3] A. L. Weisenhorn, P. K. Hansma, T. R. Albrecht, C. F. Quate, *Appl. Phys. Lett.* **1989**, *54*, 2651 – 2653.
[4] C. Bustamante, J. C. Macosko, G. J. L. Wuite, *Nat. Rev. Mol. Cell Biol.* **2000**, *1*, 130 – 136.
[5] P. Williams in *Scanning Probe Microscopies Beyond Imaging: Manipulation of Molecules and Nanostructures* (Ed.: P. Samorì), Wiley-VCH, Weinheim, **2006**, pp. 250 – 274.
[6] K. Mitsui, M. Harab, A. Ikai, *FEBS Lett.* **1996**, *385*, 29 – 33.
[7] M. Carrion-Vazquez, A. F. Oberhauser, S. B. Fowler, P. E. Marszalek, S. E. Broedel, J. Clarke, J. M. Fernandez, *Proc. Natl. Acad. Sci. USA* **1999**, *96*, 3694 – 3699.
[8] H. Li, W. A. Linke, A. F. Oberhauser, M. Carrion-Vazquez, J. G. Kerkvliet, H. Lu, P. E. Marszalek, J. M. Fernandez, *Nature* **2002**, *418*, 998 – 1002.
[9] T. R. Strick, M.-N. Dessinges, G. Charvin, N. H. Dekker, J.-F. Allemand, D. Bensimon, V. Croquette, *Rep. Prog. Phys.* **2003**, *66*, 1 – 45.
[10] J. Zlatanova, S. M. Lindsay, S. H. Leuba, *Prog. Biophys. Mol. Biol.* **2000**, *74*, 37 – 61.
[11] A. Janshoff, M. Neitzert, Y. Oberdörfer, H. Fuchs, *Angew. Chem.* **2000**, *112*, 3346 – 3374; *Angew. Chem. Int. Ed.* **2000**, *39*, 3212 – 3237.
[12] G. U. Lee, L. A. Chrisey, R. J. Colton, *Science* **1994**, *266*, 771 – 773.
[13] M. Rief, H. Clausen-Schaumann, H. E. Gaub, *Nat. Struct. Biol.* **1999**, *6*, 346 – 349.
[14] R. Krautbauer, H. Clausen-Schaumann, Hermann E. Gaub, *Angew. Chem.* **2000**, *112*, 4056 – 4059; *Angew. Chem. Int. Ed.* **2000**, *39*, 3912 – 3915.
[15] R. Krautbauer, M. Rief, H. E. Gaub, *Nano Lett.* **2003**, *3*, 493 – 496.
[16] C. Bustamante, Z. Bryant, S. B. Smith, *Nature* **2003**, *421*, 423 – 427.
[17] A. Kishino, T. Yanagida, *Nature* **1988**, *334*, 74 – 76.
[18] D. Keller, C. Bustamante, *Biophys. J.* **2000**, *78*, 541 – 556.
[19] C. Bustamante, D. Keller, G. Oster, *Acc. Chem. Res.* **2001**, *34*, 412 – 420.
[20] R. D. Vale, R. A. Milligan, *Science* **2000**, *288*, 88 – 95.
[21] I. Rayment, H. M. Holden, M. Whittaker, C. B. Yohn, M. Lorenz, K. C. Holmes, R. A. Milligan, *Science* **1993**, *261*, 58 – 65.
[22] P. Samorì, M. Surn, V. Palermo, R. Lazzaroni, P. Leclère, *Phys. Chem. Chem. Phys.* **2006**, *8*, 3927 – 3938.
[23] M. S. Z. Kellermayer, *Physiol. Meas.* **2005**, *26*, R119.
[24] S. Zou, H. Schönherr, G. J. Vancso in *Scanning Probe Microscopies Beyond Imaging: Manipulation of Molecules and Nanostructures* (Ed.: P. Samorì), Wiley-VCH, Weinheim, **2006**, pp. 315 – 353.
[25] T. Hugel, M. Seitz, *Macromol. Rapid Commun.* **2001**, *22*, 989 – 1016.
[26] T. E. Fisher, A. F. Oberhauser, M. Carrion-Vazquez, P. E. Marszalek, J. M. Fernandez, *Trends Biochem. Sci.* **1999**, *24*, 379 – 384.
[27] H. Clausen-Schaumann, M. Seitz, R. Krautbauer, H. E. Gaub, *Curr. Opin. Chem. Biol.* **2000**, *4*, 524 – 530.
[28] R. Merkel, *Phys. Rep.* **2001**, *346*, 343 – 385.
[29] P. Samorí, *J. Mater. Chem.* **2004**, *14*, 1353 – 1366.
[30] D. J. Müller, K. T. Sapra, S. Scheuring, A. Kedrov, P. L. Frederix, D. Fotiadis, A. Engel, *Curr. Opin. Struct. Biol.* **2006**, *16*, 489 – 495.
[31] F. Kienberger, A. Ebner, H. J. Gruber, P. Hinterdorfer, *Acc. Chem. Res.* **2006**, *39*, 29 – 36.
[32] T. E. Fisher, A. F. Oberhauser, M. Carrion-Vazquez, P. E. Marszalek, J. M. Fernandez, *Trends Biochem. Sci.* **1999**, *24*, 379 – 384.
[33] A. Kishino, T. Yanagida, *Nature* **1988**, *334*, 74 – 76.
[34] M. S. Kellermayer, H. I. Granzier, *Biochem. Biophys. Res. Commun.* **1996**, *221*, 491 – 497.
[35] B. Essevaz-Roulet, U. Bockelmann, F. Heslot, *Proc. Natl. Acad. Sci. USA* **1997**, *94*, 11935 – 11940.
[36] G. Binnig, C. F. Quate, C. Gerber, *Phys. Rev. Lett.* **1986**, *56*, 930.
[37] M. B. Viani, T. E. Schaffer, G. T. Paloczi, L. I. Pietrasanta, B. L. Smith, J. B. Thompson, M. Richter, M. Rief, H. E. Gaub, K. W. Plaxco, A. N. Cleland, H. G. Hansma, P. K. Hansma, *Rev. Sci. Instrum.* **1999**, *70*, 4300 – 4303.
[38] S. B. Smith, L. Finzi, C. Bustamante, *Science* **1992**, *258*, 1122 – 1126.
[39] T. R. Strick, V. Croquette, D. Bensimon, *Nature* **2000**, *404*, 901 – 904.
[40] A. Ashkin, K. Schutze, J. M. Dziedzic, U. Euteneuer, M. Schliwa, *Nature* **1990**, *348*, 346 – 348.
[41] K. Svoboda, C. F. Schmidt, B. J. Schnapp, S. M. Block, *Nature* **1993**, *365*, 721 – 727.
[42] J. Howard, A. J. Hudspeth, R. D. Vale, *Nature* **1989**, *342*, 154 – 158.
[43] M. S. Kellermayer, S. B. Smith, H. I. Granzier, C. Bustamante, *Science* **1997**, *276*, 1112 – 1116.
[44] M. D. Wang, H. Yin, R. Landick, J. Gelles, S. M. Block, *Biophys. J.* **1997**, *72*, 1335 – 1346.
[45] D. J. Müller, W. Baumeister, A. Engel, *Proc. Natl. Acad. Sci. USA* **1999**, *96*, 13 170 – 13 174.
[46] F. Oesterhelt, D. Oesterhelt, M. Pfeiffer, A. Engel, H. E. Gaub, D. J. Müller, *Science* **2000**, *288*, 143 – 146.
[47] V. T. Moy, E. L. Florin, H. E. Gaub, *Science* **1994**, *266*, 257 – 259.
[48] C. J. Liu, W. Q. Shi, S. X. Cui, Z. Q. Wang, X. Zhang, *Curr. Opin. Solid State Mater. Sci.* **2005**, *9*, 140 – 148.
[49] H. B. Li, W. K. Zhang, X. Zhang, J. C. Shen, B. B. Liu, C. X. Gao, G. T. Zou, *Macromol. Rapid Commun.* **1998**, *19*, 609 – 611.
[50] F. Oesterhelt, M. Rief, H. E. Gaub, *New J. Phys.* **1999**, *1*, 6.
[51] H. B. Li, W. K. Zhang, W. Q. Xu, X. Zhang, *Macromolecules* **2000**, *33*, 465 – 469.
[52] C. J. Liu, S. X. Cui, Z. Q. Wang, X. Zhang, *J. Phys. Chem. B* **2005**, *109*, 14807 – 14812.
[53] S. Zou, W. K. Zhang, X. Zhang, B. Z. Jiang, *Langmuir* **2001**, *17*, 4799 – 4808.
[54] Q. B. Xu, S. Zou, W. K. Zhang, X. Zhang, *Macromol. Rapid Commun.* **2001**, *22*, 1163 – 1167.
[55] Q. M. Zhang, Z. Y. Lu, H. Hu, W. T. Yang, P. E. Marszalek, *J. Am. Chem. Soc.* **2006**, *128*, 9387 – 9393.
[56] C. Wang, W. Q. Shi, W. K. Zhang, X. Zhang, Y. Katsumoto, Y. Ozaki, *Nano Lett.* **2002**, *2*, 1169 – 1172.
[57] X. Chatellier, T. J. Senden, J. F. Joanny, J. M. di Meglio, *Europhys. Lett.* **1998**, *41*, 303 – 308.
[58] L. Garnier, B. Gauthier-Manuel, E. W. van der Vegte, J. Snijders, G. Hadziioannou, *J. Chem. Phys.* **2000**, *113*, 2497 – 2503.
[59] T. Hugel, M. Grosholz, H. Clausen-Schaumann, A. Pfau, H. Gaub, M. Seitz, *Macromolecules* **2001**, *34*, 1039 – 1047.
[60] M. Conti, Y. Bustanji, G. Falini, P. Ferruti, S. Stefoni, B. Samori, *ChemPhysChem* **2001**, *2*, 610 – 613.
[61] S. X. Cui, C. J. Liu, W. Zhang, X. Zhang, C. Wu, *Macromolecules* **2003**, *36*, 3779 – 3782.
[62] S. X. Cui, C. J. Liu, X. Zhang, *Nano Lett.* **2003**, *3*, 245 – 248.
[63] M. Seitz, C. Friedsam, W. Jostl, T. Hugel, H. E. Gaub, *ChemPhysChem* **2003**, *4*, 986 – 990.
[64] S. X. Cui, C. J. Liu, Z. Q. Wang, X. Zhang, *Macromolecules* **2004**, *37*, 946 – 953.
[65] C. Friedsam, A. D. Becares, U. Jonas, M. Seitz, H. E. Gaub, *New J. Phys.* **2004**, *6*, 9.1 – 16.

[66] C. Friedsam, A. D. Becares, U. Jonas, H. F. Gaub, M. Seitz, *ChemPhysChem* **2004**, *5*, 388 – 393.
[67] C. Friedsam, M. Seitz, H. E. Gaub, *J. Phys. Condens. Matter* **2004**, *16*, S2369 – S2382.
[68] L. Sonnenberg, J. Parvole, O. Borisov, L. Billon, H. E. Gaub, M. Seitz, *Macromolecules* **2006**, *39*, 281 – 288.
[69] M. Rief, F. Oesterhelt, B. Heymann, H. E. Gaub, *Science* **1997**, *275*, 1295 – 1297.
[70] P. E. Marszalek, A. F. Oberhauser, Y. P. Pang, J. M. Fernandez, *Nature* **1998**, *396*, 661 – 664.
[71] H. B. Li, M. Rief, F. Oesterhelt, H. E. Gaub, X. Zhang, J. C. Shen, *Chem. Phys. Lett.* **1999**, *305*, 197 – 201.
[72] P. E. Marszalek, Y. P. Pang, H. B. Li, J. El Yazal, A. F. Oberhauser, J. M. Fernandez, *Proc. Natl. Acad. Sci. USA* **1999**, *96*, 7894 – 7898.
[73] P. E. Marszalek, H. B. Li, J. M. Fernandez, *Nat. Biotechnol.* **2001**, *19*, 258 – 262.
[74] Q. B. Xu, W. Zhang, X. Zhang, *Macromolecules* **2002**, *35*, 871 – 876.
[75] P. E. Marszalek, H. B. Li, A. F. Oberhauser, J. M. Fernandez, *Proc. Natl. Acad. Sci. USA* **2002**, *99*, 4278 – 4283.
[76] Z. Y. Lu, W. Nowak, G. R. Lee, P. E. Marszalek, W. T. Yang, *J. Am. Chem. Soc.* **2004**, *126*, 9033 – 9041.
[77] G. Lee, W. Nowak, J. Jaroniec, Q. M. Zhang, P. E. Marszalek, *Biophys. J.* **2004**, *87*, 1456 – 1465.
[78] Q. M. Zhang, J. Jaroniec, G. Lee, P. E. Marszalek, *Angew. Chem.* **2005**, *117*, 2783 – 2787; *Angew. Chem. Int. Ed.* **2005**, *44*, 2723 – 2727.
[79] Q. M. Zhang, G. R. Lee, P. E. Marszalek, *J. Phys. Condens. Matter* **2005**, *17*, S1427 – S1442.
[80] Q. M. Zhang, P. E. Marszalek, *Polymer* **2006**, *47*, 2526 – 2532.
[81] Q. M. Zhang, P. E. Marszalek, *J. Am. Chem. Soc.* **2006**, *128*, 5596 – 5597.
[82] K. A. Walther, J. Brujic, H. B. Li, J. M. Fernandez, *Biophys. J.* **2006**, *90*, 3806 – 3812.
[83] P. E. Marszalek, A. F. Oberhauser, H. B. Li, J. M. Fernandez, *Biophys. J.* **2003**, *85*, 2696 – 2704.
[84] R. G. Haverkamp, M. A. K. Williams, J. E. Scott, *Biomacromolecules* **2005**, *6*, 1816 – 1818.
[85] G. Lee, W. Nowak, J. Jaroniec, Q. Zhang, P. E. Marszalek, *J. Am. Chem. Soc.* **2004**, *126*, 6218 – 6219.
[86] H. B. Li, M. Rief, F. Oesterhelt, H. E. Gaub, *Adv. Mater.* **1998**, *10*, 316 – 319.
[87] W. Zhang, X. Zhang, *Prog. Polym. Sci.* **2003**, *28*, 1271 – 1295.
[88] T. E. Fisher, P. E. Marszalek, A. F. Oberhauser, M. Carrion-Vazquez, J. M. Fernandez, *J. Physiol.* **1999**, *520*, 5 – 14.
[89] M. Carrion-Vazquez, A. F. Oberhauser, T. E. Fisher, P. E. Marszalek, H. Li, J. M. Fernandez, *Prog. Biophys. Mol. Biol.* **2000**, *74*, 63 – 91.
[90] K. Wang, J. G. Forbes, A. J. Jin, *Prog. Biophys. Mol. Biol.* **2001**, *77* 1 – 44.
[91] H.-J. Butt, B. Cappella, M. Kappl, *Surf. Sci. Rep.* **2005**, *59*, 1 – 152.
[92] C. Ortiz, G. Hadziioannou, *Macromolecules* **1999**, *32*, 780 – 787.
[93] J. E. Bemis, B. B. Akhremitchev, G. C. Walker, *Langmuir* **1999**, *15*, 2799 – 2805.
[94] C. Jérôme, N. Willet, R. Jérôme, A.-S. Duwez, *ChemPhysChem* **2004**, *5*, 147 – 149.
[95] J. L. Hutter, J. Bechhoefer, *Rev. Sci. Instrum.* **1993**, *64*, 1868 – 1873.
[96] J. E. Sader, *J. Appl. Phys.* **1998**, *84*, 64 – 76.
[97] J. E. Sader, I. Larson, P. Mulvaney, L. R. White, *Rev. Sci. Instrum.* **1995**, *66*, 3789 – 3798.
[98] J. E. Sader, *Rev. Sci. Instrum.* **1995**, *66*, 4583 – 4587.
[99] J. E. Sader, J. W. M. Chon, P. Mulvaney, *Rev. Sci. Instrum.* **1999**, *70*, 3967 – 3969.
[100] J. P. Cleveland, S. Manne, D. Bocek, P. K. Hansma, *Rev. Sci. Instrum.* **1993**, *64*, 403 – 405.
[101] D. A. Walters, J. P. Cleveland, N. H. Thomson, P. K. Hansma, M. A. Wendman, G. Gurley, V. Elings, *Rev. Sci. Instrum.* **1996**, *67*, 3583 – 3590.
[102] N. Maeda, T. J. Senden, *Langmuir* **2000**, *16*, 9282 – 9286.
[103] H. J. Butt, M. Jaschke, *Nanotechnology* **1995**, *6*, 1 – 7.
[104] T. J. Senden, W. A. Ducker, *Langmuir* **1994**, *10*, 1003 – 1004.
[105] C. T. Gibson, G. S. Watson, S. Myhra, *Nanotechnology* **1996**, *7*, 259 – 262.
[106] B. T. Comella, M. R. Scanlon, *J. Mater. Sci.* **2000**, *35*, 567 – 572.
[107] J. D. Holbery, V. L. Eden, M. Sarikaya, R. M. Fisher, *Rev. Sci. Instrum.* **2000**, *71*, 3769 – 3776.
[108] J. M. Neumeister, W. A. Ducker, *Rev. Sci. Instrum.* **1994**, *65*, 2527 – 2531.
[109] J. L. Hazel, V. V. Tsukruk, *J. Tribol.* **1998**, *120*, 814 – 819.
[110] J. L. Hazel, V. V. Tsukruk, *Thin Solid Films* **1999**, *339*, 249 – 257.
[111] C. S. Hodges, *Adv. Colloid Interface Sci.* **2002**, *99*, 13 – 75.
[112] A. F. Oberhauser, P. K. Hansma, M. Carrion-Vazquez, J. M. Fernandez, *Proc. Natl. Acad. Sci. USA* **2001**, *98*, 468 – 472.
[113] B. Samorì, G. Zuccheri, P. Baschieri, *ChemPhysChem* **2005**, *6*, 29 – 34.
[114] For a review, see M. K. Beyer, H. Clausen-Schaumann, *Chem. Rev.* **2005**, *105*, 2921 – 2944.
[115] G. J. Vancso, *Angew. Chem.* **2007**, *119*, 3868 – 3870; *Angew. Chem. Int. Ed.* **2007**, *46*, 3794 – 3796.
[116] G. I. Bell, *Science* **1978**, *200*, 618 – 627.
[117] E. Evans, K. Ritchie, *Biophys. J.* **1997**, *72*, 1541 – 1555.
[118] R. G. Haverkamp, A. T. Marshall, M. A. K. Williams, *Phys. Rev. E* **2007**, *75*, 021907.
[119] M. Rief, J. M. Fernandez, H. E. Gaub, *Phys. Rev. Lett.* **1998**, *81*, 4764.
[120] F. Hanke, H. J. Kreuzer, *Eur. Phys. J. E* **2007**, *22*, 163 – 169.
[121] S. Zou, Y. Ma, M. A. Hempenius, H. Schönherr, G. J. Vancso, *Langmuir* **2004**, *20*, 6278 – 6287.
[122] M. Grandbois, M. Beyer, M. Rief, H. Clausen-Schaumann, H. E. Gaub, *Science* **1999**, *283*, 1727 – 1730.
[123] S. Cuenot, S. Gabriel, C. Jérôme, R. Jérôme, A.-S. Duwez, *Macromol. Chem. Phys.* **2005**, *206*, 1216 – 1220.
[124] S. Cuenot, S. Gabriel, R. Jerome, C. Jerome, C. A. Fustin, A. M. Jonas, A. S. Duwez, *Macromolecules* **2006**, *39*, 8428 – 8433.
[125] H. Watabe, K. Nakajima, Y. Sakai, T. Nishi, *Macromolecules* **2006**, *39*, 5921 – 5925.
[126] Y. Sakai, T. Ikehara, T. Nishi, *Appl. Phys. Lett.* **2002**, *81*, 724 – 726.
[127] W. Dettmann, M. Grandbois, S. Andre, M. Benoit, A. K. Wehle, H. Kaltner, H. J. Gabius, H. E. Gaub, *Arch. Biochem. Biophys.* **2000**, *383*, 157 – 170.
[128] P. Hinterdorfer, H. J. Gruber, F. Kienberger, G. Kada, C. Riener, C. Broken, H. Schindler, *Colloids Surf. B* **2002**, *23*, 115 – 123.
[129] A.-S. Duwez, S. Cuenot, C. Jérôme, S. Gabriel, R. Jérôme, S. Rapino, F. Zerbetto, *Nat. Nanotechnol.* **2006**, *1*, 122 – 125.
[130] N. B. Holland, T. Hugel, G. Neuert, A. Cattani-Scholz, C. Renner, D. Oesterhelt, L. Moroder, M. Seitz, H. E. Gaub, *Macromolecules* **2003**, *36*, 2015 – 2023.
[131] T. Hugel, N. B. Holland, A. Cattani, L. Moroder, M. Seitz, H. E. Gaub, *Science* **2002**, *296*, 1103 – 1106.
[132] F. Bueche, *Physical Properties of Polymers*, Interscience, New York, **1962**.
[133] G. Porod, *Monatsh. Chem.* **1949**, *80*, 251 – 255.
[134] O. Kratky, G. Porod, *Recl. Trav. Chim.* **1949**, *68*, 1106 – 1122.
[135] P. J. Flory, *Statistical Mechanics of Chain Molecules*, Hanser, München, **1898**.
[136] C. Bustamante, J. F. Marko, E. D. Siggia, S. Smith, *Science* **1994**, *265*, 1599 – 1600.
[137] J. F. Marko, E. D. Siggia, *Macromolecules* **1995**, *28*, 8759 – 8770.
[138] S. B. Smith, Y. Cui, C. Bustamante, *Science* **1996**, *271*, 795 – 799.
[139] T. Odijk, *Macromolecules* **1995**, *28*, 7016 – 7018.
[140] B. Zhang, J. S. Evans, *Biophys. J.* **2001**, *80*, 597 – 605.
[141] T. J. Senden, J.-M. di Meglio, P. Auroy, *Eur. Phys. J. B* **1998**, *3*, 211 – 216.
[142] H. Kikuchi, N. Yokoyama, T. Kajiyama, *Chem. Lett.* **1997**, 1107 – 1108.
[143] H. B. Li, B. B. Liu, X. Zhang, C. X. Gao, J. C. Shen, G. T. Zou, *Langmuir* **1999**, *15*, 2120 – 2124.
[144] W. K. Zhang, S. Zou, C. Wang, X. Zhang, *J. Phys. Chem. B* **2000**, *104*, 10258 – 10264.
[145] W. Q. Shi, S. Cui, C. Wang, L. Wang, X. Zhang, X. J. Wang, L. Wang, *Macromolecules* **2004**, *37*, 1839 – 1842.
[146] S. Zou, M. A. Hempenius, H. Schonherr, G. J. Vancso, *Macromol. Rapid Commun.* **2006**, *27*, 103 – 108.
[147] S. Zou, I. Korczagin, M. A. Hempenius, H. Schonherr, G. J. Vancso, *Polymer* **2006**, *47*, 2483 – 2492.
[148] W. Q. Shi, Z. Q. Wang, S. X. Cui, X. Zhang, Z. S. Bo, *Macromolecules* **2005**, *38*, 861 – 866.
[149] W. Q. Shi, Y. Zhang, C. Liu, Z. Q. Wang, X. Zhang, Y. Zhang, Y. Chen, *Polymer* **2006**, *47*, 2499 – 2504.
[150] L. Zhang, C. Wang, S. X. Cui, Z. Q. Wang, X. Zhang, *Nano Lett.* **2003**, *3*, 1119 – 1124.
[151] A. Scherer, C. Zhou, J. Michaelis, C. Brauchle, A. Zumbusch, *Macromolecules* **2005**, *38*, 9821 – 9825.

[152] D. Krüger, R. Rousseau, H. Fuchs, D. Marx, *Angew. Chem.* **2003**, *115*, 2353 – 2355; *Angew. Chem. Int. Ed.* **2003**, *42*, 2251 – 2253.
[153] A. J. Ryan, C. J. Crook, J. R. Howse, P. Topham, R. A. L. Jones, M. Geoghegan, A. J. Parnell, L. Ruiz-Pérez, S. J. Martin, A. Cadby, J. R. P. Webster, A. J. Gleeson, W. Bras, *Faraday Discuss.* **2005**, *128*, 55 – 74.
[154] D. Zhang, C. Ortiz, *Macromolecules* **2004**, *37*, 4271 – 4282.
[155] T. E. Fisher, P. E. Marszalek, J. M. Fernandez, *Nat. Struct. Biol.* **2000**, *7*, 719 – 724.
[156] S. Al-Maawali, J. E. Bemis, B. B. Akhremitchev, R. Leecharoen, B. G. Janesko, G. C. Walker, *J. Phys. Chem. B* **2001**, *105*, 3965 – 3971.
[157] S. Yamamoto, Y. Tsujii, T. Fukuda, *Macromolecules* **2000**, *33*, 5995 – 5998.
[158] S. Al-Maawali, J. E. Bemis, B. B. Akhremitchev, H. Y. Liu, G. C. Walker, *J. Adhes.* **2005**, *81*, 999 – 1016.
[159] B. J. Haupt, T. J. Senden, E. M. Sevick, *Langmuir* **2002**, *18*, 2174 – 2182.
[160] R. G. Haverkamp, M. A. K. Williams, J. E. Scott, *Biomacromolecules* **2005**, *6*, 1816 – 1818.
[161] C. Bouchiat, M. D. Wang, J. F. Allemand, T. Strick, S. M. Block, V. Croquette, *Biophys. J.* **1999**, *76*, 409 – 413.
[162] F. Kienberger, V. Pastushenko, G. Kada, H. J. Gruber, C. Riener, H. Schindler, P. Hinterdorfer, *Single Mol.* **2000**, *1*, 123 – 128.
[163] L. Livadaru, R. R. Netz, H. J. Kreuzer, *Macromolecules* **2003**, *36*, 3732 – 3744.
[164] A. Lamura, T. W. Burkhardt, G. Gompper, *Phys. Rev. E* **2001**, *64*, 061801.
[165] C. Storm, P. C. Nelson, *Phys. Rev. E* **2003**, *67*, 051906.
[166] T. Hugel, M. Rief, M. Seitz, H. E. Gaub, R. R. Netz, *Phys. Rev. Lett.* **2005**, *94*, 048301.
[167] P. T. Underhill, P. S. Doyle, *J. Rheol.* **2006**, *50*, 513 – 529.
[168] R. W. Ogden, G. Saccomandi, I. Sgura, *Proc. R. Soc. London Ser. A* **2006**, *462*, 749 – 768.
[169] K. Nakajima, H. Watabe, T. Nishi, *Polymer* **2006**, *47*, 2505 – 2510.
[170] H. W. Press, B. P. Flannery, S. A. Teukolsky, W. T. Vetterling in *Numerical Recipes: The Art of Scientific Computing*, Cambridge University Press, Cambridge, **1986**, p. 523.
[171] J. B. Thompson, J. H. Kindt, B. Drake, H. G. Hansma, D. E. Morse, P. K. Hansma, *Nature* **2001**, *414*, 773 – 776.
[172] E. L. Eliel, N. L. Allinger, *Topics in Stereochemistry*, Interscience, New York, **1974**.
[173] H. Li, M. Rief, F. Oesterhelt, H. E. Gaub, *Appl. Phys. A* **1999**, *68*, 407 – 410.
[174] C. J. Liu, Z. Q. Wang, X. Zhang, *Macromolecules* **2006**, *39*, 3480 – 3483.
[175] E. S. Gil, S. M. Hudson, *Prog. Polym. Sci.* **2004**, *29*, 1173 – 1222.
[176] H. J. Butt, *Macromol. Chem. Phys.* **2006**, *207*, 573 – 575.
[177] D. A. Foucher, B. Z. Tang, I. Manners, *J. Am. Chem. Soc.* **1992**, *114*, 6246 – 6248.
[178] J. Rasburn, R. Petersen, T. Jahr, R. Rulkens, I. Manners, G. J. Vancso, *Chem. Mater.* **1995**, *7*, 871 – 877.

Received: March 8, 2007
Published online on September 11, 2007

